

A NOVEL LEFT ATRIAL APPENDAGE OCCLUDER DESIGN

by

Almila Ceren Baykan

B.S., in Genetics and Bioengineering , Istanbul Bilgi University, 2015

Submitted to the Institute of Biomedical Engineering

in partial fulfillment of the requirements

for the degree of

Master of Science

in

Biomedical Engineering

Boğaziçi University

2019

**A NOVEL LEFT ATRIAL APPENDAGE OCCLUDER
DESIGN**

APPROVED BY:

Assoc. Prof. Dr. Özgür Kocatürk
(Thesis Advisor)

Assoc. Prof. Dr. Bora Garipcan

Assist. Prof. Dr. Hakan Yilmazer

DATE OF APPROVAL: 29 AUGUST 2019

ACKNOWLEDGMENTS

First and most of all, I would like to extend my sincere obligation to my advisor Assoc. Prof. Dr. Özgür Kocatürk for his guidance and patience during my thesis studies.

I am extremely thankful to Ahmet Turan Talaş and Hasan Şahin. The completion of this study could not have been possible without their support. I also would like to thank to Morteza Teymoori for his kind gesture in helping me. I also would like to mention the names of Prof. Dr. Oğuz Okay and Burak Tavşanlı from ITU Polymer Gels Research Laboratory for their help with the testing procedures.

I am greatly indebted to my friend Melisa Altınsoy and my dearest Tanzer Atay for their continuous inspirational support and understanding spirit throughout my years of study.

Finally, I owe my deepest thanks to my family for their endless support and encouragement. This accomplishment would not have been possible without them.

ACADEMIC ETHICS AND INTEGRITY STATEMENT

I, Almila Ceren Baykan, hereby certify that I am aware of the Academic Ethics and Integrity Policy issued by the Council of Higher Education (YÖK) and I fully acknowledge all the consequences due to its violation by plagiarism or any other way.

Name :

Signature:

Date:

ABSTRACT

A NOVEL LEFT ATRIAL APPENDAGE OCCLUDER DESIGN

Percutaneous left atrial appendage (LAA) occlusion is a viable nonpharmacological alternative for prevention of thromboembolic stroke in patients with atrial fibrillation (AF), especially for the patients who are unable to respond to oral anticoagulants. However, several device- or procedure-related complications were reported associated with existing implants. The aim of this study is to design and prototype a novel left atrial appendage occluder in order to prevent life-threatening complications. The proposed system allows to reduce LAA sac volume using a distal nitinol anchor while sealing the LAA ostium using a coated nitinol occluder frame. The sealing capability test of the prototyped occluder frame was performed on the phantom system mimicking left atrial with 12-30 mmHg pressure. Results have demonstrated LAA was successfully occluded and suggested that the percutaneous LAA closure with coated nitinol frame is favorable. The mechanical assessments have shown polyurethane is the promising candidate as coating material against other fabrics using in commercially available occluders. As a part of this thesis study, proof-of-concept coaxial catheter delivery system was prototyped to perform delivery and deployment of occluder frame and distal anchor, respectively. Consequently, this study presented a novel occluder design and provided a good starting point for further applications of prototyping.

Keywords: Left Atrial Appendage, Occluder, Atrial Fibrillation, Biomedical Device Design.

ÖZET

ÖZGÜN SOL ATRİYAL APENDİKS OKLÜDER TASARIMI

Perkütan yolla sol atriyal apendiksin kapatılması, özellikle oral antikoagülanlara cevap veremeyen atriyal fibrilasyonlu (AF) hastalarda, tromboembolik inmenin önlenmesinde uygulanabilir bir alternatiftir. Ancak, mevcut implantlarla ilişkili cihaz veya prosedür kaynaklı komplikasyonlar olduğu bilinmektedir. Bu çalışmanın amacı hayati tehlike oluşturan komplikasyonları önlemek için özgün bir sol atriyal apendiks oklüderi tasarlamak ve prototiplemeaktır. Sistem tasarımı, SAA girişinin polimer kaplı bir nitinol tıkayıcı kullanılarak kapatılması ardından bir distal nitinol kancası ile SAA kesesi hacminin azaltılmasını amaçlar. Oklüder sızdırmazlık testi 12 - 30 mmHg basınç aralığında sol atriyal simüle eden fantom sistemi ile gerçekleştirilmiştir. Sonuçlar sol atriyal apendiksin başarıyla tıkandığını ve polimer kaplı nitinol oklüder tasarımının perkütan SAA kapatılması prosedürünü desteklediğini göstermiştir. Mekanik değerlendirmeler poliüretanın ticari olarak temin edilebilen oklüderlerde kullanılan malzemelere kıyasla daha başarılı bir alternatif olabileceğini göstermiştir. Ayrıca, bu tez çalışması kapsamında, sırasıyla oklüder iskeleti ve distal kancanın implantasyon işlemlerini gerçekleştirmek üzere, koaksiyel kateter sistemi tasarlandı ve prototiplendi. Sonuç olarak, bu çalışma ile özgün bir oklüder tasarımı sunularak, prototip geliştirmeleri için iyi bir başlangıç noktası sağlandı.

Anahtar Sözcükler: Sol Atriyal Apendiks, Oklüder, Atriyal Fibrilasyon, Biyomedikal Cihaz Tasarımı.

TABLE OF CONTENTS

ACKNOWLEDGMENTS	iii
ACADEMIC ETHICS AND INTEGRITY STATEMENT	iv
ABSTRACT	v
ÖZET	vi
LIST OF FIGURES	ix
LIST OF TABLES	xii
LIST OF SYMBOLS	xiii
LIST OF ABBREVIATIONS	xiv
1. PREFACE	xv
2. INTRODUCTION	1
2.1 BACKGROUND	1
2.1.1 Human Heart	1
2.1.1.1 Anatomy	1
2.1.1.2 Coronary Circulation	2
2.1.1.3 Cardiac Conduction Pathway	3
2.1.2 Heart Arrhythmia	4
2.1.2.1 Long QT Syndrome (LQTS)	5
2.1.2.2 Ventricular Tachycardia (V-tach or VT)	5
2.1.2.3 Ventricular Fibrillation (VF or V-Fib)	5
2.1.2.4 Supraventricular Tachycardia	6
2.1.2.5 Atrial Flutter	6
2.1.2.6 Atrial Fibrillation (AF or A-Fib)	6
2.1.3 Atrial Fibrillation and Stroke	7
2.1.4 Left Atrial Appendage (LAA)	8
2.1.5 Current Solutions	10
2.1.5.1 Anticoagulation	10
2.1.5.2 Surgical Excision or Exclusion	11
2.1.5.3 Percutaneous Transcatheter Occlusion	12
2.1.6 Current Complications	18

2.1.6.1	Perforation of the LA or LAA	18
2.1.6.2	Occluder Embolism	19
2.1.6.3	Thrombus Formation on Occluder	19
2.1.7	Biomedical Device Design Concept	19
2.1.8	Medical Textiles	22
2.1.8.1	Braiding Technology of Medical Textiles	22
2.1.8.2	Horizontal Braiding Machine	23
2.1.9	Nitinol	23
2.1.9.1	Shape Setting with Heat Treatment	24
2.1.10	Polyurethane	24
2.2	OBJECTIVE	27
3.	METHOD	28
3.1	Design and Prototyping	28
3.1.1	3D Anatomical Model	31
3.1.2	Occluder Frame and Distal Anchor	34
3.1.3	Coating of the Nitinol LAA Occluder Frame	40
3.1.4	The Delivery System of the Nitinol LAA Closure Device	42
3.1.5	In Vitro LAA Phantom	45
3.2	Testing Procedure	48
3.2.1	Tensile Test	48
3.2.2	Shear Test	49
3.2.3	Sealing Test	50
4.	RESULTS	52
5.	DISCUSSION	56
6.	CONCLUSION AND FUTURE WORKS	58
	REFERENCES	60

LIST OF FIGURES

Figure 2.1	Heart anatomy [1].	2
Figure 2.2	Internal heart anatomy [2].	2
Figure 2.3	The electrical conduction pathway of the heart [3].	4
Figure 2.4	ECG tracing of ventricular fibrillation [4].	6
Figure 2.5	Comparison of atrial flutter and A-fib mechanisms [4].	6
Figure 2.6	ECG tracing of atrial fibrillation [4].	7
Figure 2.7	Variation in LAA morphologies [5].	9
Figure 2.8	Frontal and lateral 3D representation of the four main classes of LAA morphologies [6].	9
Figure 2.9	ArtiClip LAA exclusion system [7].	12
Figure 2.10	Endopath endoscopic linear cutter [8].	13
Figure 2.11	Endoscopic linear cutter surgery procedure [9].	13
Figure 2.12	PLAATO device [10].	14
Figure 2.13	AMPLATZER Cardiac Plug [11].	14
Figure 2.14	AMPLATZER Septal Occluder [12].	15
Figure 2.15	AMPLATZER Amulet [11].	15
Figure 2.16	WATCHMAN device [13].	16
Figure 2.17	LARIAT Suture Delivery System (Image courtesy of SentreHeart, Inc.).	17
Figure 2.18	Thrombus formation on occluder [14].	19
Figure 2.19	Waterfall model of design controls for medical devices.	20
Figure 2.20	Biomedical device design phases.	21
Figure 2.21	Horizontal braiding machine.	24
Figure 2.22	Phase transformation by change in temperature.	25
Figure 2.23	Phase transformation by stress.	25
Figure 2.24	Scheme of the prepolymerization used for the preparation of polycarbonate-based polyurethanes [15].	26
Figure 3.1	Drawing of delivery system placement.	28
Figure 3.2	Drawing of nitinol self-expanding LAA occluder mesh deployment.	29

Figure 3.3	Drawing of the nitinol distal anchor disc deployment.	29
Figure 3.4	Drawing of completed procedure.	30
Figure 3.5	A sample digital heart anatomical model.	31
Figure 3.6	Digital heart anatomical model-2.	32
Figure 3.7	Hollowed digital LAA anatomical model.	32
Figure 3.8	(a) AUTOCAD Meshmixer, (b) Zortrax M200 Desktop 3D Printer.	32
Figure 3.9	3D printed heart (with LAA) models.	33
Figure 3.10	3D printed hollowed LAA model.	33
Figure 3.11	Silicone LAA models.	34
Figure 3.12	Braided, heat-treated nitinol.	35
Figure 3.13	One layer disc form.	35
Figure 3.14	Two layer disc form.	36
Figure 3.15	Manual braiding trials.	36
Figure 3.16	Occluder frame with round nitinol wires.	37
Figure 3.17	The aluminum mold used for shape setting procedure of round and flat nitinol wires with sharp distal ends.	37
Figure 3.18	The OmniCure LX 400+ UV light source machine.	38
Figure 3.19	(a) Shaped flat nitinol wire. (b, c, d) Occluder frame with flat nitinol wires.	38
Figure 3.20	Occluder frame with curved end flat nitinol wires.	39
Figure 3.21	6-leaf (left) and 3-leaf (right) clover-shaped distal nitinol anchor trials.	39
Figure 3.22	The aluminum mold used for shape setting procedure of distal anchor structure.	40
Figure 3.23	Silicone-coated proximal disc of nitinol occluder frame.	41
Figure 3.24	Polyurethane-coated proximal disc of nitinol occluder frame.	41
Figure 3.25	PTFE mold designed for fully coating of occluder frame.	42
Figure 3.26	Fully silicone-coated nitinol occluder frame.	42
Figure 3.27	(a) Inner delivery catheter, (b) Middle fixed catheter, (c) Outer delivery catheter.	43
Figure 3.28	(a) Illustration of external view of the control handle, (b) Illustration of internal view of the control handle.	43

Figure 3.29	The components of the control handle.	44
Figure 3.30	Nitinol occluder frame encapsulated in the distal end of the outer catheter.	44
Figure 3.31	The demonstration of deployed occluder components on the delivery catheters.	45
Figure 3.32	The complete delivery system.	45
Figure 3.33	Functional block diagram of the components of the heart phantom.	46
Figure 3.34	The overall picture of the in vitro LAA phantom: (a) Peristaltic pump, (b,e) Pressure sensors, (c) Silicone left atrium heart model, (d) Amplifier circuit and micro-controller.	46
Figure 3.35	(a) 3D-printed heart model, (b) Silicone anatomical model.	47
Figure 3.36	Dimensions of the dog-bone tensile test specimen.	48
Figure 3.37	Tensile test setup (Zwick Roell zwickiLine).	49
Figure 3.38	Polyurethane coated nitinol specimens.	50
Figure 3.39	(a) Encapsulated thrombus-like structures in LAA model (b) Silicone-coated occluder appearance after fitting into LAA ostium.	51
Figure 4.1	The tensile test results.	52
Figure 4.2	Shear test results.	53
Figure 4.3	Images obtained during shear test procedure of silicone-coated nitinol specimen at 5, 20 and 40 seconds, respectively.	53
Figure 4.4	Images obtained during shear test procedure of polyurethane-coated nitinol specimen at 5, 20 and 40 seconds, respectively.	54
Figure 4.5	Real-time pressure values of sealing test procedure.	54
Figure 4.6	Images of (a) the complete anatomical heart model and (b) the LAA part of the anatomical model obtained at the end of the 15 minutes sealing test procedure.	55
Figure 4.7	Images of front (a) and side (b) views of the reduced LAA sac by volume.	55

LIST OF TABLES

Table 2.1	CHA ₂ DS ₂ -VASc stroke risk assessment score table.	11
Table 2.2	Advantages and disadvantages of LAA occlusion procedures [16].	18



LIST OF SYMBOLS

<i>KPa</i>	Kilopascal
<i>F</i>	French, catheter scale
<i>NiTi</i>	Nitinol
<i>mm</i>	Milli-meters, metric unit
<i>mmHg</i>	Milli-meters of Mercury, manometric unit
$^{\circ}C$	Degree Celsius
μm	Micro-meters, metric unit
cm^3	Volume in metric system

LIST OF ABBREVIATIONS

3D	3 Dimensional
AF	Atrial Fibrillation
AV	Atrioventricular
CE	European Conformity
CVD	Cardiovascular Disease
DAPT	Dual Antiplatelet Therapy
ECG	Electrocardiogram
FDA	Food and Drug Administration
LA	Left Atrial
LAA	Left Atrial Appendage
LQTS	Long QT Syndrome
MI	Myocardial Infarction
NVAF	Non-valvular Atrial Fibrillation
OAC	Oral Anticoagulation
PEEK	Polyether Ether Keton
PEN	Polyethylene Naphthalate
PET	Polyethylene Terephthalate
PLAATO	The Percutaneous Left Atrial Appendage Transcatheter Occlusion
PP	Polypropylene
PTFE	Polytetrafluoroethylene
SA	Sinoatrial
SVT	Supraventricular Tachycardia
TIA	Transient Ischemic Attack
V-Fib	Ventricular Fibrillation
V-Tach	Ventricular Tachycardia
VF	Ventricular Fibrillation
VT	Ventricular Tachycardia

1. PREFACE

In chapter 2, human heart anatomy and related arrhythmia diseases were discussed. Among these diseases atrial fibrillation and its relation with stroke was examined in more detail. In this regard the role of the left atrial appendage structure was evaluated. The solutions applied to occlude an LAA with conventional commercial occluder device types, and their working principles, as well as current complications encountered during the occlusion of LAA were discussed. Additionally, the objectives of this thesis study were elaborated to plan a proper method to design, and prototype a device and tools for the occlusion of LAA.

In chapter 3, the device design and prototyping steps were described including previous iterations of the occluder device which is the main part of the whole procedure. Coating trials and related material selection were mentioned. System designs to support the delivery and deployment process of the occluder were included. Preparation of basic 3D models and heart phantom for use in operational testing of the device were discussed. In addition, tensile, shear and sealing test procedures were stated.

In chapter 4, all the results of tensile tests of silicone and polyurethane, and shear tests of silicone-nitinol and polyurethane-nitinol conducted with material testing device for comparison of their adhesion, and also sealing test conducted with designed phantom were discussed.

In chapter 5, results were discussed. Summary of the achievements were mentioned.

In chapter 6, modifications planned to design and prototype a new LAA occluder device were mentioned as the future work.

2. INTRODUCTION

2.1 BACKGROUND

2.1.1 Human Heart

The heart is a muscular organ providing continuous blood circulation in human body. It is a muscle functioning to transfer the deoxygenated blood from the tissues to the lungs and to pump oxygenated blood into the body. By this circulation, the human heart provides nutrients and oxygen to the organs, including itself, while removing carbon dioxide and other cellular wastes.

2.1.1.1 Anatomy. Human heart (illustrated in Figure 2.1) is located in the thoracic cage and composed of four chambers: right atrium, left atrium, right ventricle and left ventricle. Two upper chambers are named as atria and two lower chambers are named as ventricles, which are thicker-walled and stronger to pump blood. There are 4 valves in the heart that maintain one-way flow: Tricuspid and bicuspid atrioventricular (AV) valves, pulmonary and aortic semilunar valves [2].

There is a continuous two-layered serous fluid filled cover surrounding heart. This membrane is called pericardium. The surface of the pericardium in contact with heart is called visceral pericardium or epicardium and the other surface is called parietal pericardium. There is a layer called myocardium which is a muscle tissue of heart wall beneath the pericardium. This tissue consists of cardiac muscle cells network, aligned circular and spirally, to direct the flow of blood. These muscle cells have ion channels on their surfaces. The electrical activity of the heart occurs when the cells triggered by Ca^{2+} ions and the ion channels open and close with allowing the transition of sodium potassium and calcium ions. The inner layer of heart is the endocardium lining of the atrial and ventricular chambers as well as arteries and veins. The endocardium also

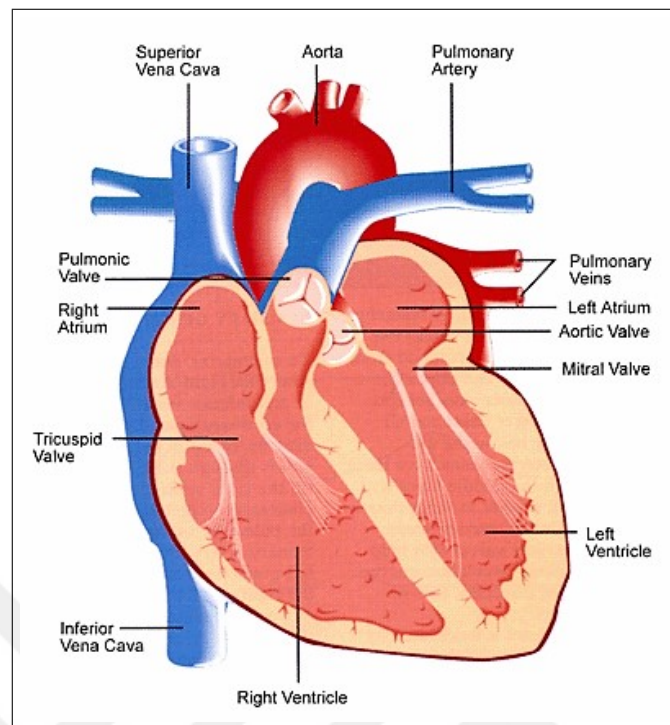


Figure 2.1 Heart anatomy [1].

surrounds the surfaces of the valves [2].

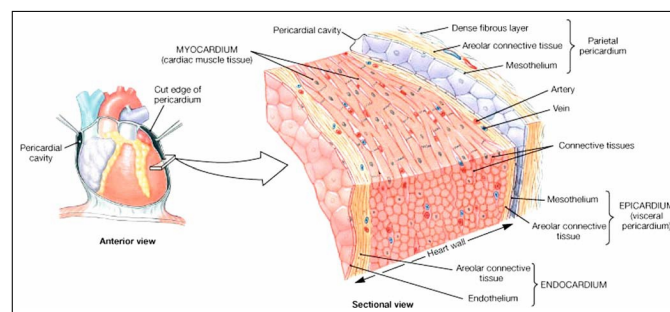


Figure 2.2 Internal heart anatomy [2].

2.1.1.2 Coronary Circulation. The blood delivered to the lungs for oxygenation by the right side of the heart and transmitted to the left side of the heart. First, it passes through the left atrium, which is a thin wall structure chamber, and then it is transmitted to collect in the left ventricle chamber with thicker walls. The left atrium and ventricle are divided by called mitral valve that allows blood transition. This transition is due to the pressure difference between the two chambers. Since the pressure in the left ventricle is lower than left atrial during diastole (relaxation)

phase, the mitral valve opens and provides blood flow. Accumulated blood in the left ventricle is transmitted to the aorta by contraction and then to the tissues with capillaries. The deoxygenated blood returning from the tissues reaches the right atrium by the venous system. The right atrium is thin walled, similar to the left atrium. The blood accumulated in the right atrium is filled into the right ventricle through the tricuspid valve. The principles of the contraction of the right ventricle and the left ventricle are similar. However, the right ventricle is thinner-walled to generate less pressure due to the fact that it transfers blood to the lungs instead of pumping blood to the whole body like the left ventricle. At the final stage the blood oxygenated in the lungs turns to the left atrium and completes the circulation. Left ventricle driven blood circulation is called systemic circulation and right ventricle driven blood circulation is called pulmonary circulation [17].

2.1.1.3 Cardiac Conduction Pathway. The cardiac cycle is a set of mechanical activities are regulated by electrical activities of myocardium. The heart has the ability to contract by nerve cells without the need for external stimulation. In this way, the heart can create its own rhythm and, in doing so, generate the electrical impulses that follow the specific path.

The sinoatrial (SA) node, which is a special heart muscle node in the right atrium wall, is capable of the fastest contractions. SA node cells are more susceptible to Na^+ ions than other heart muscle cells, so they are very rapidly depolarized and initiate heart beat (60-80 beats per minute). The contraction pulses move from the SA node to the atrioventricular (AV) node. The AV bundle is located in the upper interventricular septum. The AV node transmits the pulses to the right and left bundle branches. The transmitted electrical pulses travel along the Purkinje fibers and produce ventricular systoles [3]. These electrical activities on the heart can be visualized on the electrocardiogram (ECG). The locations of these nodes and conduction pathway are shown in Figure 2.3.

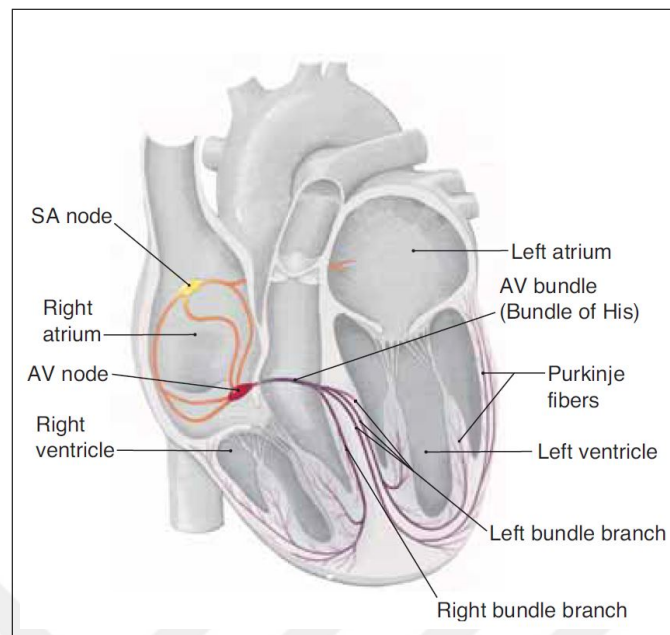


Figure 2.3 The electrical conduction pathway of the heart [3].

In cases where the SA node did not work properly, the AV node may initiate a heart beat. However, this creates a heart rate at a much lower rate (50 to 60 beats per minute). In addition, in some heart diseases where impulse conduction is blocked, the AV node may produce a rhythm of the ventricle at very low rates (15 to 40 beats per minute) [3].

2.1.2 Heart Arrhythmia

In normal conditions, the heart contracts and relaxes with regular rhythm. Abnormal rhythm of the heart is known as arrhythmia (dysrhythmia). This rhythm may be slower or faster than normal or may be completely irregular. If it beats too fast, it is called tachycardia or if it beats too slow, it is called bradycardia. Arrhythmias can usually be harmless. However, it may have serious or fatal consequences according to the causes. Arrhythmia can be examined in 6 different classes: Long QT syndrome, ventricular tachycardia, ventricular fibrillation, supraventricular tachycardia, atrial flutter, and atrial fibrillation [18].

2.1.2.1 Long QT Syndrome (LQTS). Long QT syndrome is observed as a result of impaired electrical activity due to improper operation of ion channels or small amount of them found on the surfaces of heart muscle cells. It usually is inherited, although it can also be acquired. LQTS can be diagnosed by electrocardiogram (ECG), genetic tests, physical exams, and medical and family history. It can be recognized by T-wave abnormalities and QT prolongation on the ECG and can be treated by surgery, medical devices such as pacemakers, medicines or even lifestyle changes depend on the type of LQTS [19].

2.1.2.2 Ventricular Tachycardia (V-tach or VT). Ventricular tachycardia is a continual fast beating of the ventricles, the lower chambers of heart. A small number of beats of ventricular tachycardia usually do not cause any problems. However, if it takes more than a few seconds it can cause serious consequences. It can become ventricular fibrillation (v-fib) which is more dangerous arrhythmia. It is caused by abnormal electrical signals in the ventricles. During VT heart often beats more than 100 times in a minute and it does not sync with the atrial chambers. This causes the heart to be unable to pump enough blood into the body and lungs since the chambers cannot fill properly. In patients with another heart problem such as heart attack history or cardiomyopathy, VT can be the reason of sudden cardiac arrest [18].

2.1.2.3 Ventricular Fibrillation (VF or V-Fib). Ventricular fibrillation (shown in Figure 2.4) is the most dangerous cardiac arrhythmia. It occurs because of the unorganized, chaotic electrical activity of the heart. It can be caused by ventricular tachycardia or ischemic heart disease. These lead the formation of ventricular complexes occurring simultaneously with a T wave on the ECG. It can either be with acute myocardial infarction (MI) or without it. If it causes MI, instant defibrillation is the necessary treatment [20].

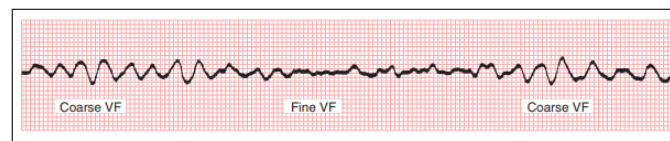


Figure 2.4 ECG tracing of ventricular fibrillation [4].

2.1.2.4 Supraventricular Tachycardia. Any arrhythmia that needs atrial or atrioventricular gateway tissue for its initiation is supraventricular tachycardia. They are known by 100 or more beats per minute. It can be separated into irregular rhythms and the atria and ventricles can beat at different rates. Atrial flutter and atrial fibrillation are types of SVT [21].

2.1.2.5 Atrial Flutter. Atrial fluttered heart has 250 to 350 beats per minute. The signal that maintains the upper chambers beating can be interrupted due to harmed tissue. The signal, large reentrant wave tries to create another path, and this can cause a counterclockwise direction loop (in Figure 2.5) and repeated atria beating. Some of these repeated beats are transmitted to the ventricle, while others produce extra beats in the atrium. This causes the atria and the ventricles to beat in different rates [22].

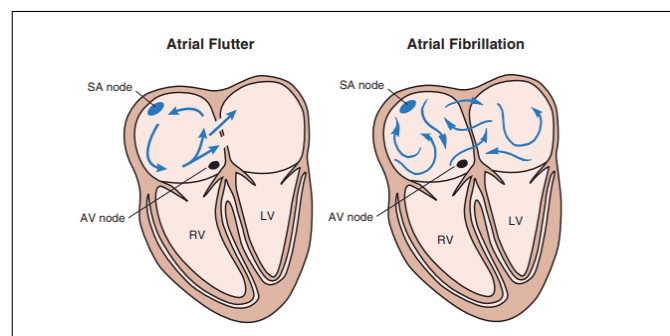


Figure 2.5 Comparison of atrial flutter and A-fib mechanisms [4].

2.1.2.6 Atrial Fibrillation (AF or A-Fib). The most common cardiac rhythm disturbance (arrhythmia) is named atrial fibrillation (in Figure 2.6) and caused by erratic electrical activities and weak upper chamber contraction of the heart. It is

a disease with the consequences of cardiovascular morbidity and mortality. Several studies show it affects 0.8-2% of the population [23] and incidence of AF increases with age. 25% of people aged >40 years have risk of developing AF. However, AF can remain undiagnosed for a long period of time due to silent nature of itself [24]. Different populations of all ethnic groups were studied in terms of gender. Accordingly, it is documented that men are with a higher prevalence in all age groups [5]. However, there are still many epidemiological uncertainties as there are significant differences between study results.



Figure 2.6 ECG tracing of atrial fibrillation [4].

2.1.3 Atrial Fibrillation and Stroke

Atrial fibrillation was accepted as a stroke risk factor after studies showed an independent relation between them; a five-fold increase in stroke occurrence is seen in patients with atrial fibrillation. Also, it is considered that 15% of all strokes can be associated with AF [25]. For the reason that AF develops mainly because of heart diseases, increased stroke incidences are linked to cardiovascular disease (CVD) rather than AF. In spite of that, showing more than two-thirds of the strokes can be prevented by anticoagulation, which has a great effect in preventing atrial thrombus formation, has strengthened the importance of AF [26].

There are certain distinctions between the stroke etiologies. Patients with rheumatic valvular heart disease have stroke risk linked to left atrial thrombogenicity and left atrial thrombus formation. 31% of stroke risk is related with AF, and 8% of it is without recorded AF. On the other hand, stroke history, increasing age, female

gender, transient ischaemic attack, or systemic embolism can be the risk factors of AF related stroke [5].

Despite, vascular diseases such as coronary artery disease, peripheral arterial disease, myocardial infarction cause increase in AF-related stroke, the root of stroke is usually the embolism of the cardiac thrombus [25]. Therefore, it has also long been recognized that structural heart disease is associated with stroke observation in patients with AF.

2.1.4 Left Atrial Appendage (LAA)

Researches indicate that the 90% of the atrial thrombus in nonvalvular AF, 47% of the atrial thrombus in valvular AF formed in the left atrial appendage [27], which is a round, hollow, hook-like structure and a protrusion in the left atrium. LAA structure for regular beating hearts usually does not cause a problem. The LAA is filled with blood like the left atrium when the heart relaxes, and it transfers the blood to the left ventricle when heart contracts. If the atrium does not effectively contract as in atrial fibrillation, the LAA structure causes blood to become a clot. Then embolization of these clots to the brain become a reason of a stroke. Like the appendix in the gastrointestinal tract is not an abnormal part, LAA is also not an abnormal part of the heart anatomy. However, the function of LAA is still unknown.

LAA morphology and internal anatomy vary considerably (shown in Figure 2.7) among patients. Its size ranges between 0.77-19.27 cm³ in volume, 5-27 mm in short diameter and 10-40 mm in long diameter [28]. Even so, shape of LAA is categorized into general types: chicken wing, windsock, cauliflower and cactus (in Figure 2.8).

Although there are differences in the morphologies of LAA, its position in the left atrium and relationship with the mitral valve, pulmonary veins, and coronary arteries are basically the same. This provides a principle for performing LAA procedures. However, these differences in LAA morphologies require careful imaging of LAA and

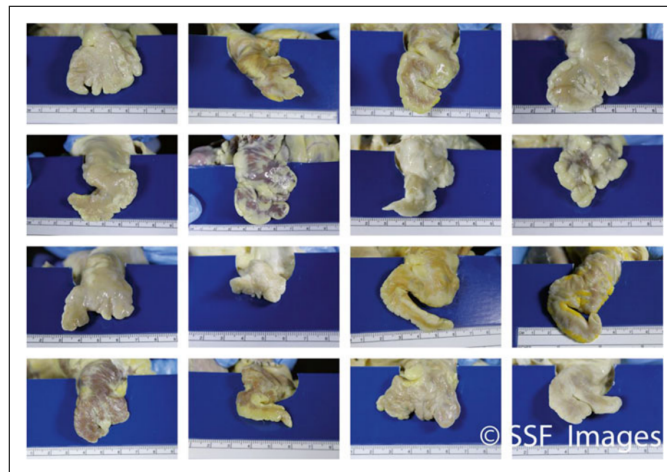


Figure 2.7 Variation in LAA morphologies [5].

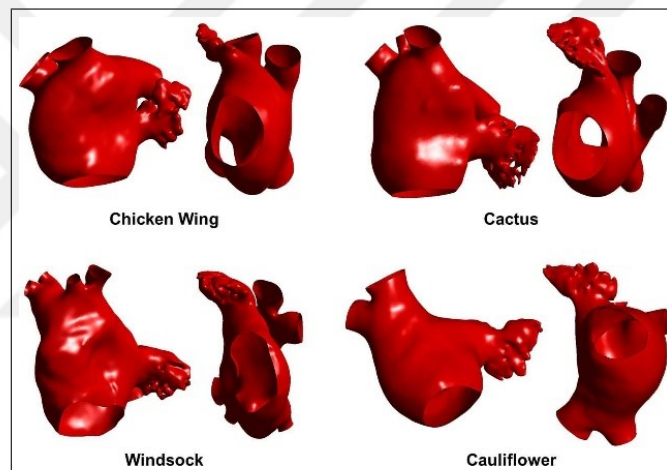


Figure 2.8 Frontal and lateral 3D representation of the four main classes of LAA morphologies [6].

surrounding structures, and prior planning for each procedure.

There are 5 anatomical parts related with LAA. Atrial septum is one of them. This part moves with atrial expansion and has fossa ovalis, which is a structure that allows blood to pass from right atrium to left atrium during fetal development. It plays an important role in the delivery of the catheter to left atrial. Mitral valve, which is located inferior anterior, and left pulmonary vein, which is located posterior to LAA, define the borders of LAA ostium. Circumflex artery and cardiac vein, and phrenic nerve in the surrounding tissues of LAA, are the other structures that can be damaged and cause complications during the transcatheter occlusion procedure [5]. In addition,

LAA can be examined in 4 parts in order to plan the procedure correctly. Ostium is the entrance of LAA defined by left pulmonary vein and mitral valve. Neck is the segment between the ostium and body of LAA. Lobes are the structures that cause LAA to be studied in various morphology classes. Finally, there are pectinate muscles that are the trabeculated myocardial network of LAA. Although it is rare, they can cause a misdiagnosis due to the conjecture as a thrombus [29].

2.1.5 Current Solutions

LAA tend to form thrombus due to its complex anatomical structure, numerous cavities and low blood flow during AF. Studies using imaging techniques such as magnetic resonance and transesophageal echocardiography have shown that having larger LAA ostium, more cavities and longer LAA body all represent a higher risk of stroke [30].

Currently, the strategy for stroke prevention can be provided in several ways: oral systemic anticoagulation, surgical techniques, and transcatheter techniques. However, efficacy of these approaches can be discussed depend on their individual advantages and disadvantages.

2.1.5.1 Anticoagulation. First-line therapy for preventing stroke in AF patients is oral anticoagulation such as receiving warfain and also apixaban, dabigatran and rivaroxaban (next-generation anticoagulants), which are more effective in decreasing stroke incidence and systematic embolism [27]. Anticoagulant use is determined by the CHADS₂ stroke risk assessment tool. Physicians using CHADS₂ score for risk assessment can make more precise decisions about the advantages and risks of initiating anticoagulation therapy. Also, it is recommended that applying CHA₂DS₂-VASc score (shown in Table 2.1) for the patients have lower values of CHADS₂ score in order to evaluate further risk.

Table 2.1
CHA₂DS₂-VASc stroke risk assessment score table.

Condition	0	+1	+2
Congestive Heart Failure(CHF) History	No	Yes	-
Hypertension History	No	Yes	-
Age	<65	65-74	>74
Diabetes Mellitus History	No	Yes	-
Stroke/TIA/Thromboembolism History	No	-	Yes
Vascular Diseases History	No	Yes	-
Sex	Male	Female	-

Although oral anticoagulants are accepted as gold standard treatment of stroke prevention in patients with atrial fibrillation, the risk of intracranial haemorrhage in patients receiving warfarin (oral anticoagulant) is 5-fold higher, especially for older patients [31].

2.1.5.2 Surgical Excision or Exclusion. The left atrial appendage (LAA) has been called as most lethal human attachment [32]. Excision or exclusion procedures are recommended to practice under coronary artery bypass, mitral valve or aortic valve replacement surgery of AF patients. However, incomplete LAA closure is seen about 60% of the cases and increases stroke risk up to 24% [33].

AF patients with incomplete closure need to receive anticoagulants which is reverse of the main purpose of procedure. Besides, suturing techniques frequently leaves a suture line on the endocardial surface which can cause thrombus formation and stapling methods can harm the LAA tissue [34]. Even there are limitations in guidelines about surgical exclusion of LAA, there are devices produced to remove LAA.

AtriClip LAA Exclusion System

The AtriClip LAA Exclusion System (Atricure, West Chester, OH) shown in Figure 2.9 is a woven polyester fabric covered titanium ring. Clip is placed around the base of the LAA by using a deployment tool, under direct visualization. After clip deployment

by using Deployment Tab, deployment tool is removed, clip and attachment suture is left behind. It is important to position the clip carefully to prevent tissue damages; after pulling the Deployment Tab, the device cannot be used for repositioning [35].



Figure 2.9 ArtiClip LAA exclusion system [7].

Endoscopic Linear Cutter

Endoscopic Linear Cutter (Ethicon Endo-Surgery, Cincinnati, OH) shown in Figure 2.10 is advanced via the left lateral thorax, with minimally invasive thoracoscopic procedure. In the beginning of the procedure left lung is deflated. Cutter removes LAA with closing the base of it which is shown in Figure 2.11.

The most important disadvantages of this procedure are the risks of lung deflation and the potential of bleeding into a closed chest [36].

2.1.5.3 Percutaneous Transcatheter Occlusion. Although new generation anticoagulants have lower risk of bleeding than warfarin, some of them have increased risk of gastrointestinal bleeding. Unfortunately, there are also AF patients who are unable to respond to anticoagulants. Percutaneous LAA occlusion is a viable nonpharmacological alternative in such cases, and also a good alternative to avoid the morbidity of open surgery of exclusion. It is a safe and cost-effective procedure for preventing stroke in patients with non-valvular AF (NVAf) with the risk of stroke and bleeding.



Figure 2.10 Endopath endoscopic linear cutter [8].

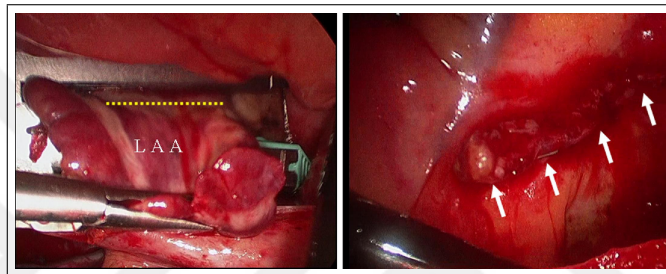


Figure 2.11 Endoscopic linear cutter surgery procedure [9].

To occlude the left atrial appendage via transcatheter delivery, several occluder types have been designed by different companies.

Percutaneous Left Atrial Appendage Transcatheter Occlusion

The Percutaneous Left Atrial Appendage Transcatheter Occlusion (PLAATO) (Figure 2.12) is the first percutaneous left atrial appendage occluder and it is no longer available since 2006. It has a 15-32 mm nitinol cage with polytetrafluoroethylene (PTFE) cover. The cage is self-expanding and PTFE membrane is blood impermeable. Small anchors provide anchoring to the LAA tissue. It occludes the ostium of the LAA and allows tissue generation. Delivery of the device is provided by 12-14 F trans-septal sheath via venous and trans-septal puncture. The delivery system allows repositioning or complete removal of the device in case of undesired events [37].

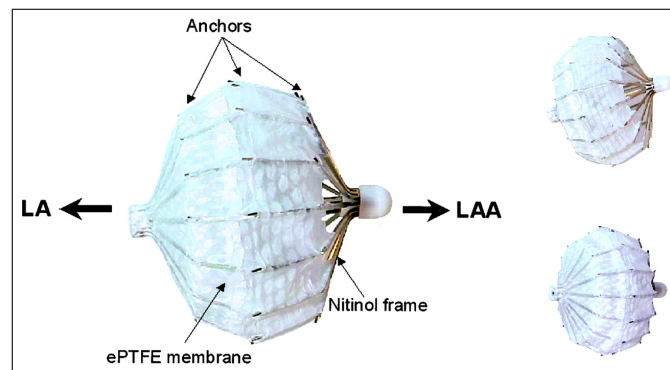


Figure 2.12 PLAATO device [10].

AMPLATZER Cardiac Plug and Amulet

The AMPLATZER cardiac plug (St. Jude Medical, Plymouth, MN) (Figure 2.13) is an updated version of AMPLATZER Septal Occluder (Figure 2.14) redesigned for the LAA occlusion. It is a 16-30 mm self-expanding braided nitinol with a polyester patch. It is delivered trans-septally into LAA through 9-13 F sheath. The distal part of the device is for preventing migration, and proximal part is for occlusion of the ostium [27].



Figure 2.13 AMPLATZER Cardiac Plug [11].

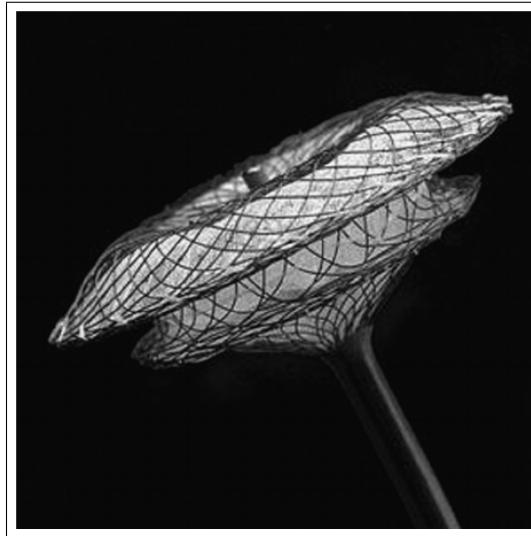


Figure 2.14 AMPLATZER Septal Occluder [12].

A second-generation device of the AMPLATZER named Amulet (shown in Figure 2.15) is with design improvements such as larger size and having additional stabilizing wires provides successful occlusion of LAA anatomies. Studies that compare two AMPLATZER devices have indicated similar results about implantation success, safety, and appropriate LAA occlusion [38].



Figure 2.15 AMPLATZER Amulet [11].

WATCHMAN

The WATCHMAN LAA Closure Device (Boston Scientific, Marlborough, MA) was designed by inspiration from PLAATO device (Figure 2.16). It has a self-expanding nitinol cage with 160 μm polyethylene terephthalate (PET) and anchors for providing fixation. PET membrane(Dacron) covers atrial face of the device and provides endothelialization [38]. Due to its permeable structure, anticoagulation procedure is required at least 6 weeks until device endothelialization. It is available in 5 sizes: 21 mm to 33 mm. and delivery of the device is performed by 14 F sheath and standard trans-septal puncture.



Figure 2.16 WATCHMAN device [13].

Studies have shown that after implantation of WATCHMAN device, achieving improvement in quality-of-life with termination of daily taking anticoagulants, less bleeding problems, and dietary-drug interaction problems [39]. However, studies also have reported short- and long-term complications such as periprocedural stroke, pericardial effusion, incomplete sealing of LAA, device embolization and device thrombus formation [40].

LARIAT

LARIAT is a LAA occlusion system with 12 F suture delivery device used to tie off the LAA and delivered by using 0.025-inch and 0.035-inch opposite-pole, magnet-tipped guide wires (in Figure 2.17).

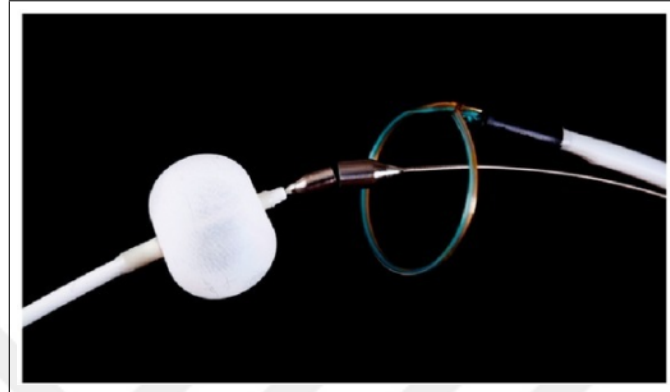


Figure 2.17 LARIAT Suture Delivery System (Image courtesy of SentreHeart, Inc.).

It is a minimally invasive technique and does not leave foreign material inside cardiac chamber. The LARIAT device has a 15mm diameter balloon catheter with 9 F delivery tool for occlusion of the ostium to prevent adverse events of damaging the LAA tissue that cause bleeding during the procedure. It also serves as a marker. One of the two magnet-tipped guide wires is placed inside of the LAA through a trans-septal sheath, and the other is positioned into the epicardial space through a subxiphoid puncture to bind each other [41].

All the above mentioned devices have advantages and disadvantages due to designs, specifications and application procedures and these are summarized in Table 2.2.

Table 2.2
Advantages and disadvantages of LAA occlusion procedures [16].

	Advantages	Disadvantages
Surgical Excision or Exclusion	<ul style="list-style-type: none"> - No device part left in body - Standard procedure for every LAA morphology 	<ul style="list-style-type: none"> - Open surgery - Bleeding or leak - Residual LAA remnant - Lack of data on post-procedural medicational treatments
Percutaneous Transcatheter Occlusion	<ul style="list-style-type: none"> - Trans-septal access only - Long-term satisfying results of clinical trials - Evaluated medication treatments after procedure 	<ul style="list-style-type: none"> - Anatomic exclusion - Possible leak - Possible device thrombus - Possible device embolization
Transcatheter Ligation	<ul style="list-style-type: none"> - Standard size device for every LAA morphology - No device part left in body 	<ul style="list-style-type: none"> - Anatomic exclusion - Pericardial access - Possible leak - Possible remnant thrombus - Lack of data on post-procedural medicational treatments

2.1.6 Current Complications

There are several complications likely to occur related with above-mentioned percutaneous occlusion devices and procedures, during or after the procedure.

2.1.6.1 Perforation of the LA or LAA. There may occur some device-related or procedure-related life-threatening complications such as pericardial effusion and perforation during the LAA occlusion procedure. These can be related to device deployment by advancing each of the instruments: occluder, sheath and guidewire. Also, repeated implantation attempts can cause multiple punctures. Although there are usually no problems in the procedures performed by mostly experienced surgeons, surgical intervention may be required in case of a complication. For this reason, it is important to design the device and delivery system, and to plan the procedure depending on the device specifications in a way that does not cause complications [42].

2.1.6.2 Occluder Embolism. Device embolization caused by migration is one of the complications of percutaneous transcatheter closure of LAA. This circumstance is mostly related with the device type and size. Oversizing or undersizing the device can increase the migration risk. Another potential reason of device embolism is acute change in intracardiac pressure [14]. Therefore, it is important to use the correct imaging techniques in order to detect the right position of the device and arrange the best surgical approach during the operation.

2.1.6.3 Thrombus Formation on Occluder. Thrombus formation on LAA occlusion devices (illustrated in Figure 2.18) is frequent and related with a higher risk of strokes and TIA during follow-up. Clinical conditions such as older age and ischemic stroke history are important for prediction of device-related thrombus. For early diagnosis of thrombus caused by devices, active screening is important after implantation. Dual Antiplatelet Therapy (DAPT) and Oral Anticoagulation (OAC) at discharge are also important to lower risk of thrombus formation on the device.

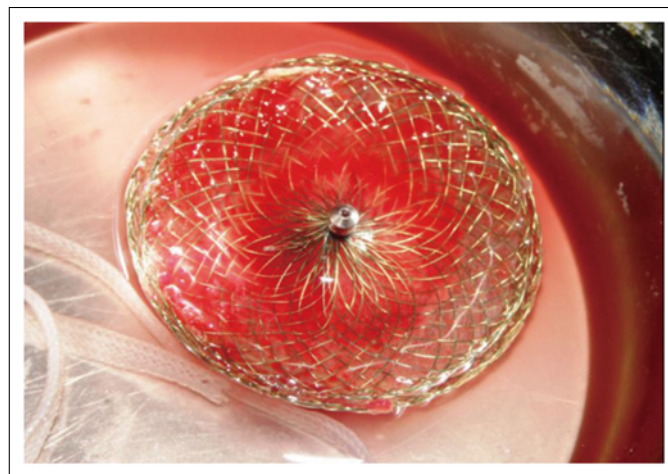


Figure 2.18 Thrombus formation on occluder [14].

2.1.7 Biomedical Device Design Concept

Device design process is the most important phase for the success of a medical device development. For a medical device to be marketed, it must be correctly

defined and designed to meet all the regulatory requirements stated by the governing organizations such as FDA, CE etc. Otherwise, it would fail to provide benefits and functionality that are the needs of the market and suffer from less market acceptance compared to well designed competitor products. Consequently, the main purpose of the medical device design process is to ensure that a new design meets user expectations and that it is safe and effective in providing the claimed benefits. In addition, the fact that a medical device has direct interaction with human body makes the design process much more sensitive and requires a thorough consideration of stages such as material selection.

There is a waterfall model (Figure 2.19) of FDA in Design Control Guidance for Medical Device Manufacturers in order to clarify the design process[43]. With this model, validation and verification concepts can be understood better.

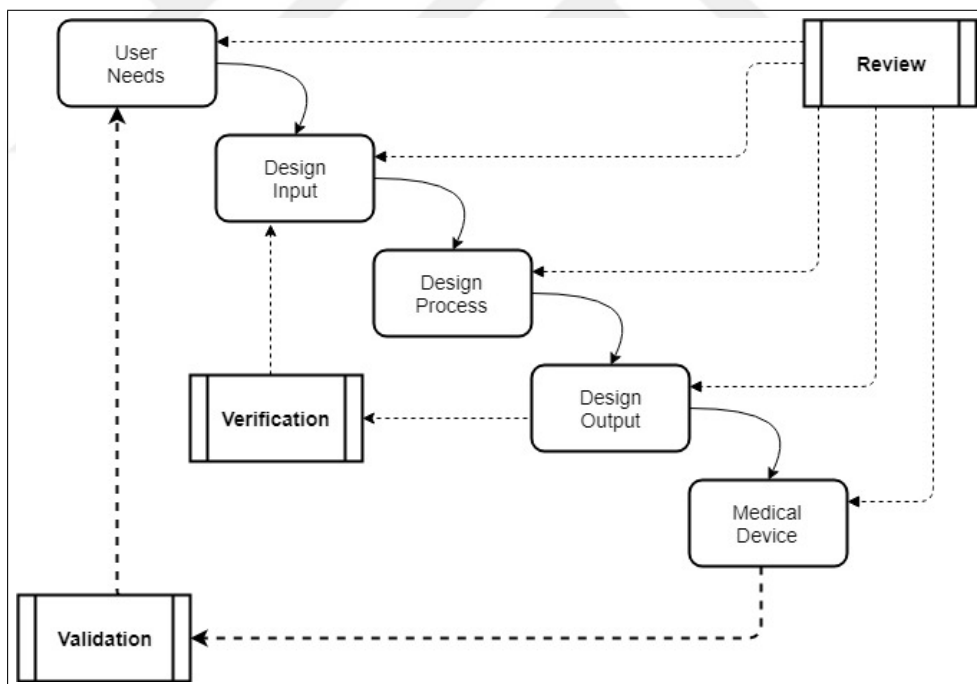


Figure 2.19 Waterfall model of design controls for medical devices.

Based on this model, the conformity of verification to the requirements is provided with the comparison of design input and design output. Verification is much more detailed examination. On the other hand, validation is a cumulative summation of all efforts, including verification.

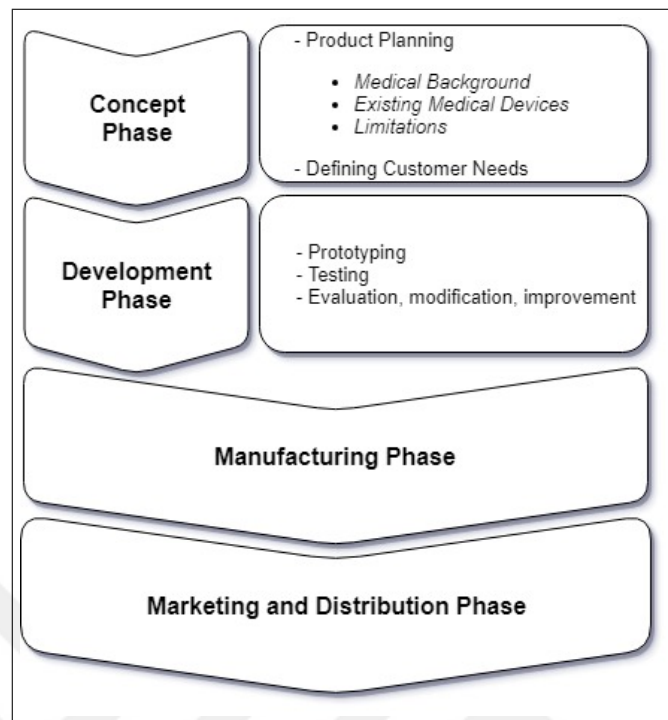


Figure 2.20 Biomedical device design phases.

The concept phase (Figure 2.20) usually starts with product planning. Correct definition and documentation of the medical device design is important. This planning is usually done by design engineers. They need to have product specific market knowledge. At this stage, product-specific clinical application information should be obtained, competing products in the market should be examined and limitations should be correctly defined. Then the requirements of the customers should be identified and documented. It is crucial to understand the exact need that is to be solved with the new product at the beginning of this phase. Therefore, finding the right experts is necessary. In case of medical devices knowledge should be acquired from the physician specializing in this area which are the end users of the designed product [44].

The development phase is a complex and critical phase of the medical device development. The requirements of hardware, software, mechanical design specifications are created and approved in this phase. As the waterfall chart in the Figure 2.19, review and verification are required for ensuring that design meets the proper requirements. Then, engineering prototypes are developed. This progress should be validated by documentation and revision control procedures. Device prototypes are tested extensively

according to related standards to prove if the design meets the hardware, software, production or marketing requirements and addresses the respective risks. The tests performed according to requirement specifications is called verification. Proof of conformity according to the intended use is called validation. In case of any undesired result of the tests, the design can be modified or changed. Clinical testing, regulatory or governmental clearances are the critical tasks which are also initiated in the development phase [45].

In manufacturing phase, design engineers has to work close for scale-up. They need to ensure that mass-produced product meets the design requirements and be comparable with prototypes.

Clinical use of the medical devices is only possible after the successful completion of the phases mentioned above and obtaining FDA or CE clearance.

This study includes applications from the concept and the development phase for a novel design of LAA occluder.

2.1.8 Medical Textiles

Medical textile products are classified as medical devices range from simple bandage materials or sutures to tissue culture and a wide range of implants. They are preferred due to their textile properties such as softness, lightness, flexibility, absorption and filtration. These products must also meet the requirements expected from medical devices. Since they are more sensitive than normal textile products, braiding technologies and devices need to be more sensitive and special [46].

2.1.8.1 Braiding Technology of Medical Textiles. Today's medical device manufacturers needs go beyond traditional braiding processes. New braiding technologies offer a wide range of braiding products, from stents, occluders, mesh-reinforced tubes

to endoscope and catheter knits. Thanks to these technologies, besides the production of multi-channel fine wire mesh, the strength of the pipes can be increased while reducing the size of the pipes. These braiding technologies include braiding machines for the production of surgical sutures, stents and catheters. Horizontal-extra-fine wire mesh has been developed particularly for small lumen stents, catheters and occluders with Nitinol wire. Braiding machines with high-quality and new technology can process even very thin wires from 0.1 mm to 20 mm in diameter at high speeds. Since these machines have interchangeable braiding bodies, the number of braiding bodies varies from 3 to 48 carriers. Braidings in the medical field are made with 24, 32, 48, 64, 80, 96 or 144 wires. However, 85% of the produced knits have 16 to 48 wires. In addition to all these, enclosed and oil-free production makes braiding machines suitable for use in clean rooms [47].

2.1.8.2 Horizontal Braiding Machine. The placement of braiding heads in the horizontal braiding machine (Steeger, SC, USA) is shown in Figure 2.21. With this system, stainless steel, copper, NiTi (Nitinol), Titanium, Platinum, Cobalt Chromium and coated wires can be braided over the specimen. The machine can also braid non-metallic monofilament fibers such as Nylon, PET, PEN, PP, PEEK. The round wire/fiber size ratio ranges from 0.0005 inches to 0.010 inches [48].

2.1.9 Nitinol

Nitinol is a shape memory alloy composed of Nickel and Titanium components. The key properties of nitinol are superelasticity, shape memory and biocompatibility. Due to these properties, it has become an important material for medical device engineers in cardiovascular, neurovascular, endovascular and orthopedics areas.

Shape memory and superelastic properties of nitinol are caused by reversible solid-state phase transformations. These phase transformations take place from austenite to martensite or vice versa (Figure 2.22). Phase transformation by change in tem-

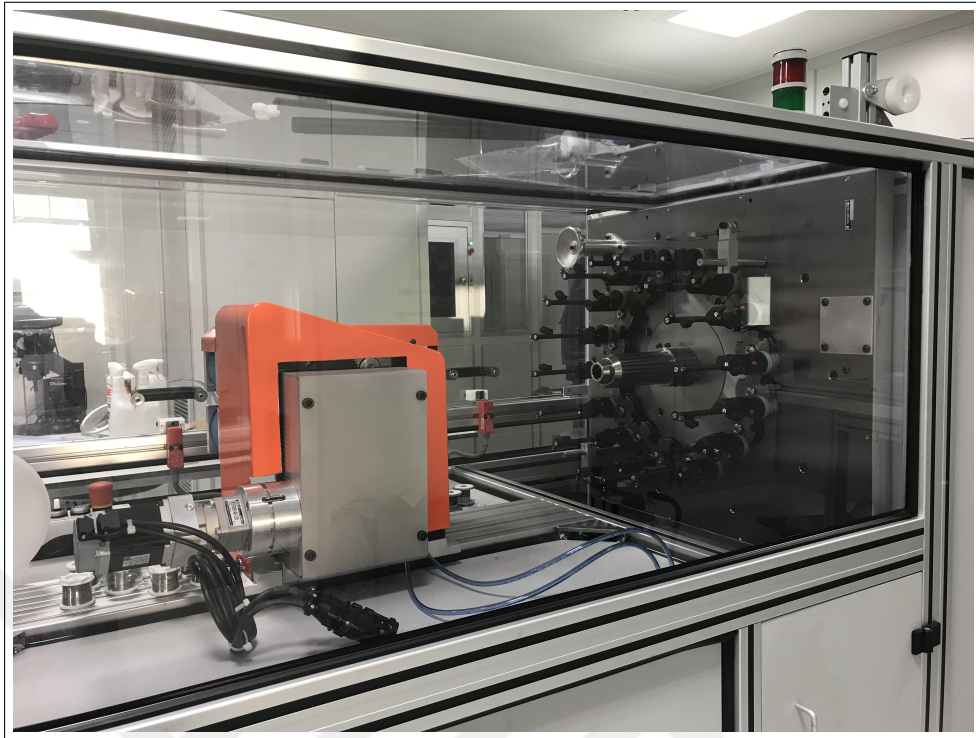


Figure 2.21 Horizontal braiding machine.

perature is responsible for shape memory and by stress is for superelasticity (Figure 2.23).

2.1.9.1 Shape Setting with Heat Treatment. Shape setting is the process of configuring the transformational and mechanical properties of nitinol. This process requires heat treatment application using special equipments. Shape setting recommendations include temperature ranges between 470 to 550 °C. Actual temperature and application times are determined by the starting alloy composition and the desired thermal and mechanical properties. This shaping process is usually finished with a water immersion to prevent further aging and reduce process variability [49]. [0,10]

2.1.10 Polyurethane

Polyurethanes are one of the most commonly used polymers for medical device production due to its biocompatibility, performance, and ease of production.

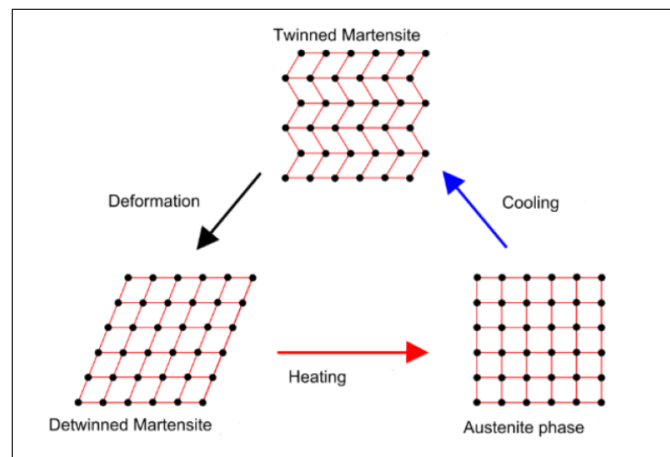


Figure 2.22 Phase transformation by change in temperature.

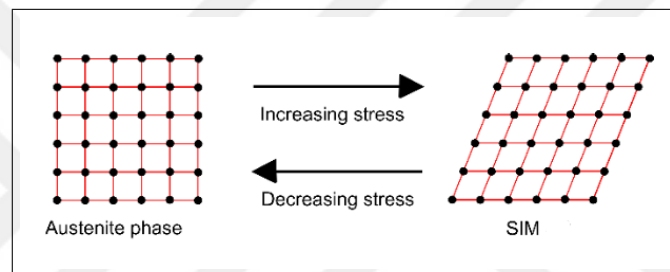


Figure 2.23 Phase transformation by stress.

Polyurethanes are polymers containing blocks of high-molecular-weight polyols linked together by a urethane group. Due to the polyol structure and cross-link characteristics, they can show rigid, semirigid, or flexible properties. In addition to their biocompatibility, hydrolytic stability, abrasion resistance, physical strength and high flexure endurance, they also resist to gamma radiation, oils, acids and bases [50].

Polyurethane elastomers are made up of linear primary polymer chains (shown in Figure 2.24) which are combination of relatively long, flexible, soft-chain segments that have been joined end to end with rigid, hard-chain segments through covalent chemical bonds. Soft segments are coupled with diisocyanate for use in medical applications [50].

Segmented polyurethane elastomers have been used in long-term implantable devices since 1960s. However, only poly(ester)urethanes that are first generation

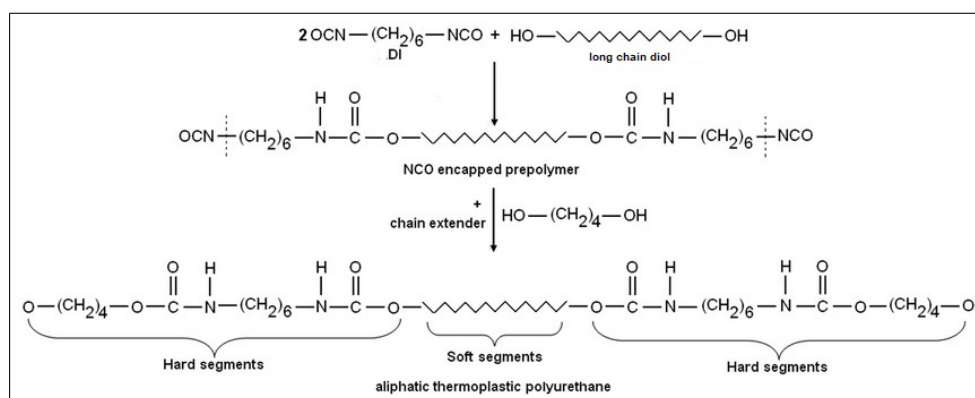


Figure 2.24 Scheme of the prepolymerization used for the preparation of polycarbonate-based polyurethanes [15].

polyurethanes were available until 1970s. It was understood that they were unsuitable for long-term implantation due to their rapid hydrolysis by the endogenous enzymes under the warm and humid condition. Because of their poor hydrolytic stability, polyester-based polyurethanes have not been used in durable medical implants [51].

Second-generation polyurethanes are poly(ether)urethanes. This kind of polyurethanes were accepted as hydrolytically stable and were able to be used for long-term medical devices due to their mechanical strength, low moisture absorbance and also low coefficient of friction. However, even the poly(ether)urethane ether linkage was hydrolytically stable, it was shown to be sensitive to *in vivo* oxidation, particularly when subjected to mechanical stresses [51].

Oxidative stability of poly(carbonate)urethanes was led to replacement of poly(ether)urethanes in 1980s. Poly(carbonate)urethanes are preferred polymers for long-term implants due to their properties such as biodegradability [51].

For all these reasons, poly(carbonate)urethanes are preferred and used as biodegradable implants instead of poly(ester)urethane or poly(ether)urethane.

2.2 OBJECTIVE

Nitinol occluder devices are needed to conduct interventional treatment procedures for LAA of heart occlusion to prevent clot transition in circulatory system caused stroke events. In line with the constraints mentioned in previous chapter, there are many challenges existing.

Commercially available occluder devices used as LAA closure devices cannot provide complete sealing and cannot prevent possible leakage led by the presence of LAA volume mostly due to size variation between patients and therefore novel design ideas are needed.

The main objective of this study is to introduce a novel occluder design that can reduce the LAA sac volume in addition to sealing the LAA ostium by elimination of all the challenges such as clot formation and the risk of embolic event caused by the device. In addition, ensuring that occluder parts are composed of materials with smooth surfaces to eliminate the potential formation of thrombus in clinical use.

After completing the final design, proposed design prototypes were tested in vitro phantom.

3. METHOD

In this chapter, the design and fabrication stages of three dimensional (3D) heart models, occluder frame, distal anchor, coating, delivery system and phantom will be explained in detail with drawings and visuals. In addition, test procedures for testing the prototypes will be discussed.

3.1 Design and Prototyping

The proposed occluder design can be delivered to the LAA, the target location, using a delivery system with at least 2 coaxial catheters. One of them will carry the nitinol mesh which provides sealing and will be placed in the ostium region, while the other will carry the nitinol anchor which will be placed on the exterior surface of the LAA after puncturing it to reduce the LAA sac volume. Overall implant and delivery system will be introduced. First, the overall delivery system will be placed into the LAA region (shown in Figure 3.1) through septal puncture from the right side under X-ray fluoroscopy.

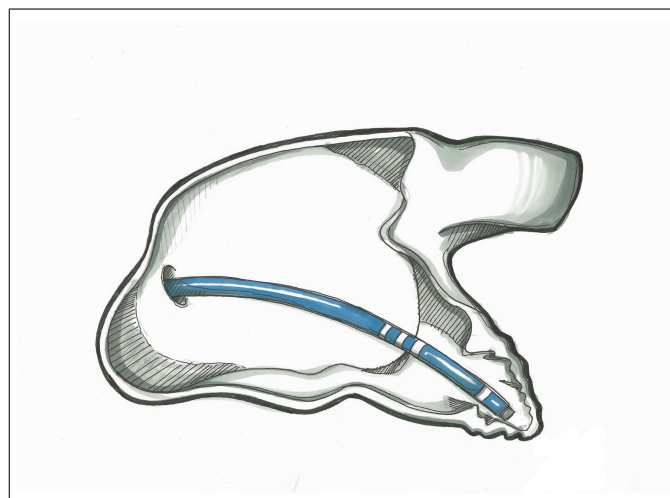


Figure 3.1 Drawing of delivery system placement.

The deployment procedure shown in Figure 3.2 of the self-expanding nitinol LAA occluder design covered with fabric.

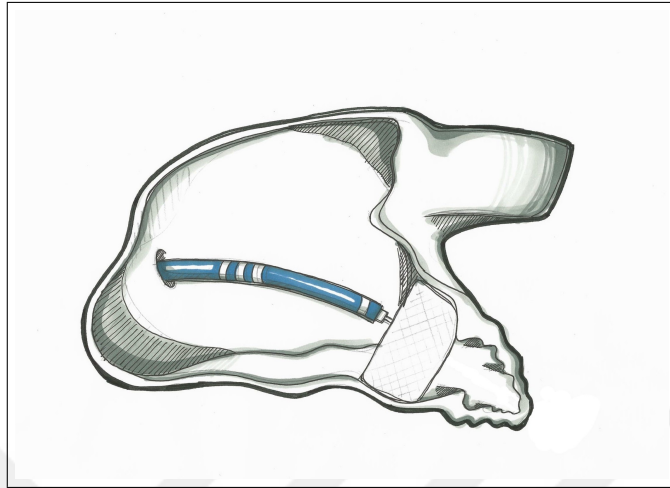


Figure 3.2 Drawing of nitinol self-expanding LAA occluder mesh deployment.

The nitinol anchor will then be deployed between the 2 layers of the pericardial membrane of the heart to form a disc (shown in Figure 3.3). This procedure aims to minimize the complications such as blood clot dislodgement from LAA during any adverse event caused by perforation.

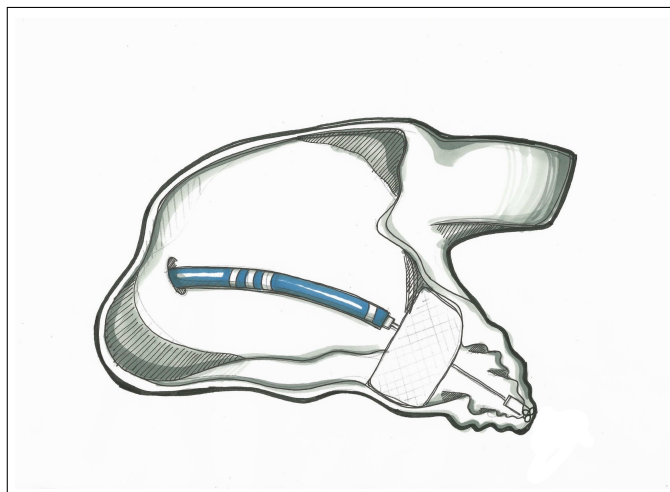


Figure 3.3 Drawing of the nitinol distal anchor disc deployment.

After the deployment, when the nitinol anchor is pulled, it will reduce the LAA sac volume. Finally, by bringing the two nitinol components together, the device will be left in the desired position and the delivery system will be pulled to complete the interventional procedure (in Figure 3.4).

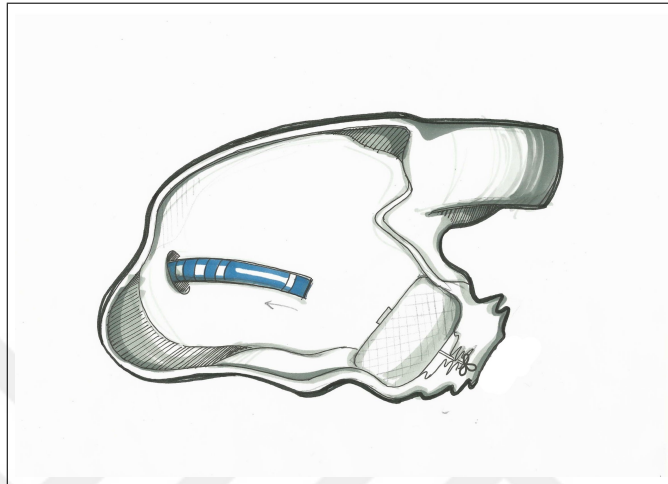


Figure 3.4 Drawing of completed procedure.

The appearance of LAA after placing and securing the proposed LAA closure device design.

A novel LAA occluder device must address design constraints of the complex morphology of the left atrial appendage while implementing design inputs in order to improve outcomes over commercial devices.

During the delivery procedure, catheters must be deliverable through vessels with minimum resistance, and through septal puncture with minimum damage. The 14 Fr \pm 2 delivery catheter can be acceptable for initial designs [52].

The self-expanding occluder provides better deliverability with a lower crossing profile. Balloon-expandable systems require internal expansion balloons which increase crossing profiles compared with self-expanding systems. Deformation of more than 10% strain can be elastically recovered by some materials, and this behavior is called superelasticity [53]. A superelastic material should be preferred in order to design a self-expanding occluder components. The self-expanding occluder frame should be 25

± 5 mm in diameter [52]. In addition, using thinner sizes of material will support the aim of providing a lower crossing profile.

Materials should be chosen and treated to form smooth surfaces in order to prevent tissue damage. There should also be strong adhesion between the metal alloys and the coating polymer. Additionally, the coating polymer should be biocompatible, biodurable and tough. Biodurability is needed for preventing corrosion-associated adverse events such as toxic effects of metals and loss of mechanical strength. The overall device also must exhibit corrosion resistance, biocompatibility, and must be low in thrombogenicity. Blood interaction tests should be performed depend on ISO 10993-4. However, there is no accepted criteria from FDA or ASTM for corrosion rate [54].

3.1.1 3D Anatomical Model

Due to variation in size and shape between patients, a thorough understanding of the physical structure of the LAA is critical to identifying design parameters. The related digital heart anatomical models (shown in Figure 3.5, 3.6 and 3.7) have been important for our design process.

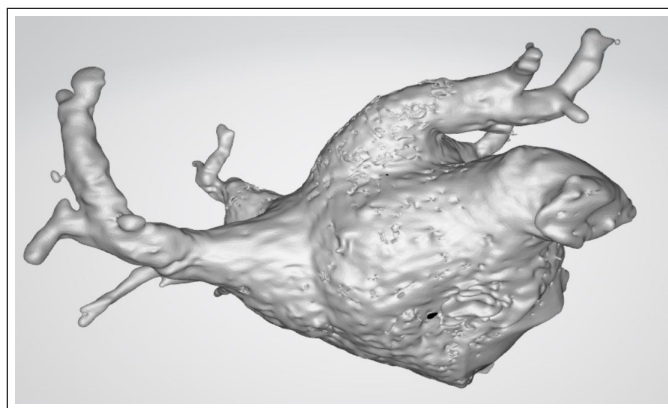


Figure 3.5 A sample digital heart anatomical model.

Two different 3D heart models have been formed using a 3D Printer (Zortrax M200 Desktop) as shown in Figure 3.8 (b).

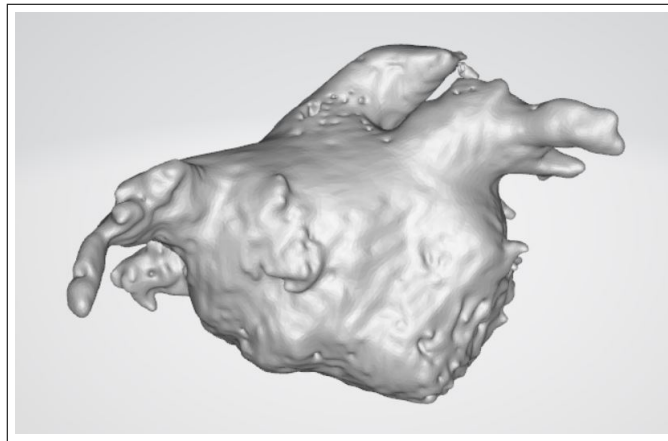


Figure 3.6 Digital heart anatomical model-2.

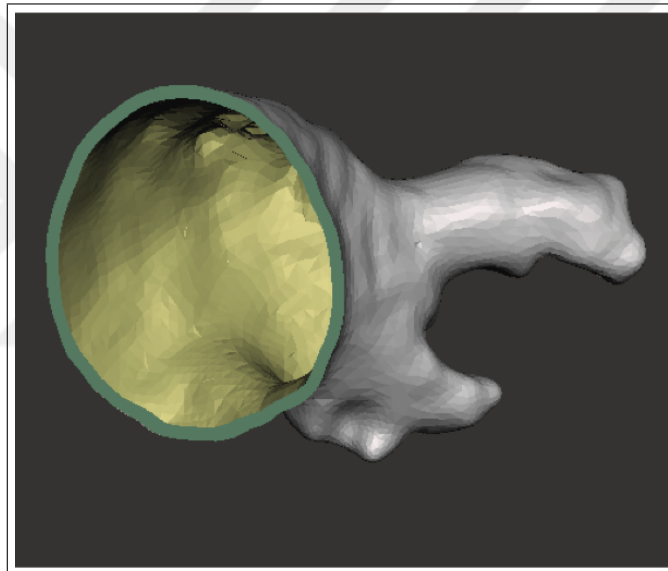


Figure 3.7 Hollowed digital LAA anatomical model.

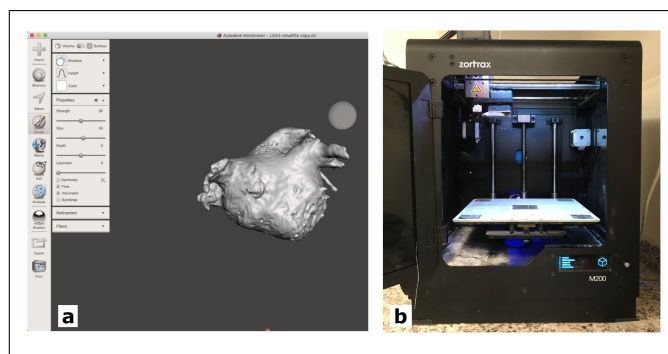


Figure 3.8 (a) AUTOCAD Meshmixer, (b) Zortrax M200 Desktop 3D Printer.

First, AUTOCAD Meshmixer (shown in Figure 3.8 (a)) program was used to make necessary modifications on digital models before 3D printing process (Figure 3.9 and Figure 3.10).

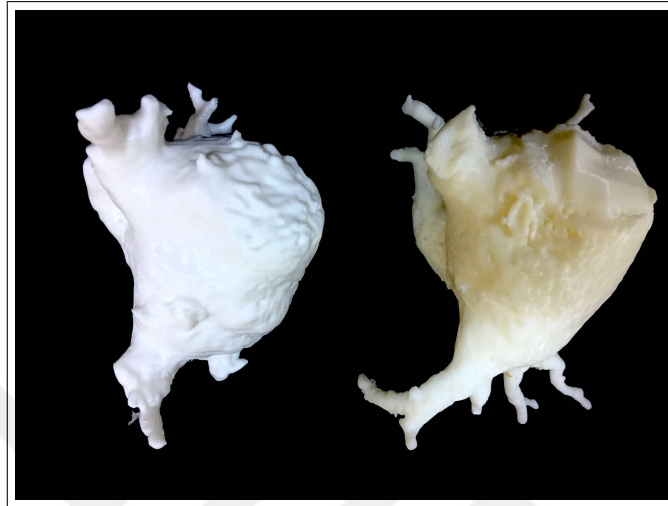


Figure 3.9 3D printed heart (with LAA) models.



Figure 3.10 3D printed hollowed LAA model.

3D printed LAA models used as mold to prepare silicone LAA models (Figure 3.11).

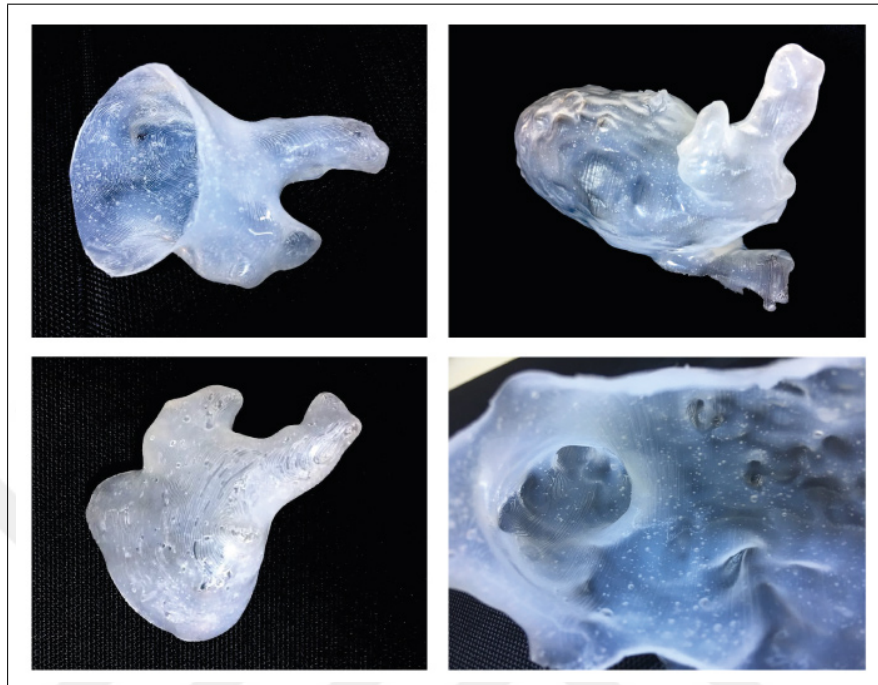


Figure 3.11 Silicone LAA models.

3D printed LAA models were coated with silicone (Mold Star™ 20T, Smooth-on Inc.). The silicone elastomers come with A and B components were mixed in a one-to-one ratio by volume. The silicone was applied on the 3D heart models by brush that was expected to self-spread and to become a smoother surface during in cure time for 30 minutes.

3.1.2 Occluder Frame and Distal Anchor

Several LAA occluder designs were evaluated to finalize the design.

The first LAA occluder design was performed by using braided nitinol shown in Figure 3.12. For this purpose, nitinol wires with a diameter of 0.005 inches were used which was braided on a 23 mm diameter mandrel and then shape set with heat treatment.

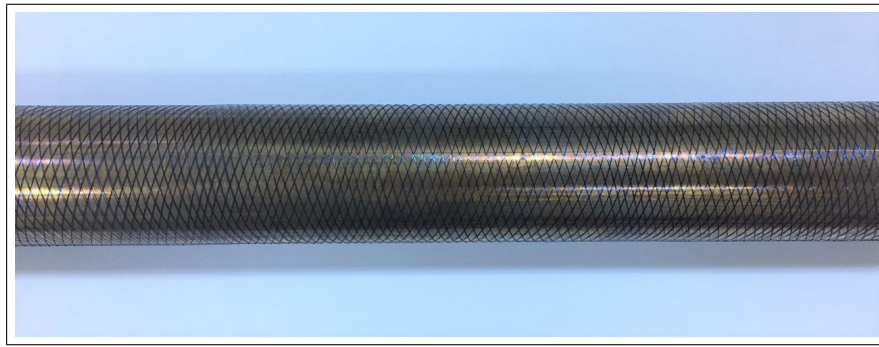


Figure 3.12 Braided, heat-treated nitinol.

Once the braided nitinol was heat treated, it was constrained between two aluminum blocks machined via 3 axis CNC system (NAAS Automation) to form a disc-like shape (shown in Figure 3.13) and put through the heat treatment process once more.

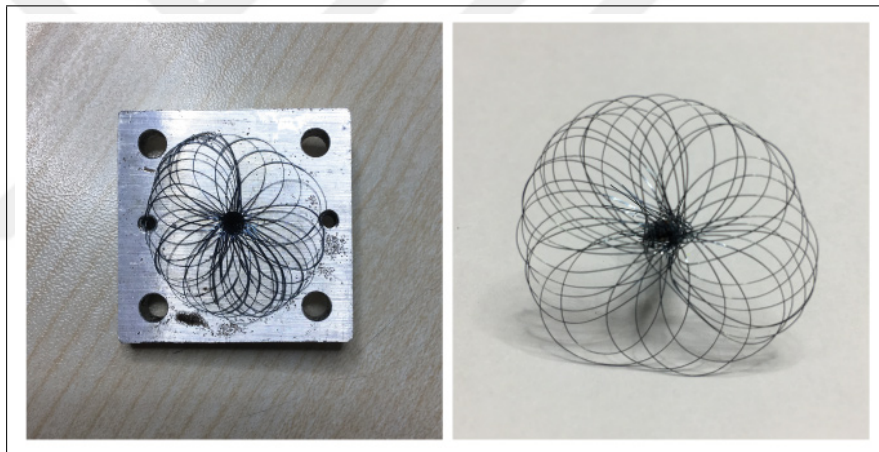


Figure 3.13 One layer disc form.

The purpose of this flat disc-like shape was to provide a good adhesion surface for the coating and consequently seal the ostium part of LAA while preventing thrombus formation on the occluder.

In order to increase the nitinol mesh density of the occluder frame, a double-layer disc was formed using the same method (in Figure 3.14).

Further enhancement of the mesh density in the occluder frame was sought by using manual braiding methods. Figure 3.15 shows the custom-made braiding molds developed using the 3D printer.

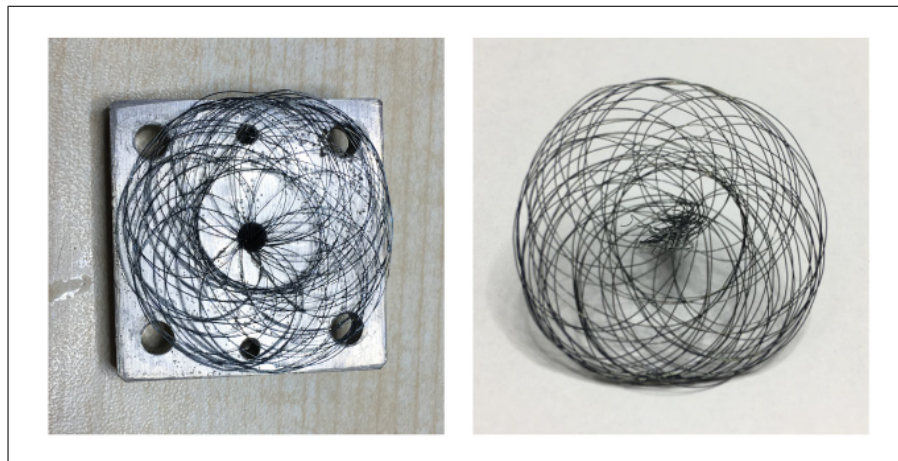


Figure 3.14 Two layer disc form.

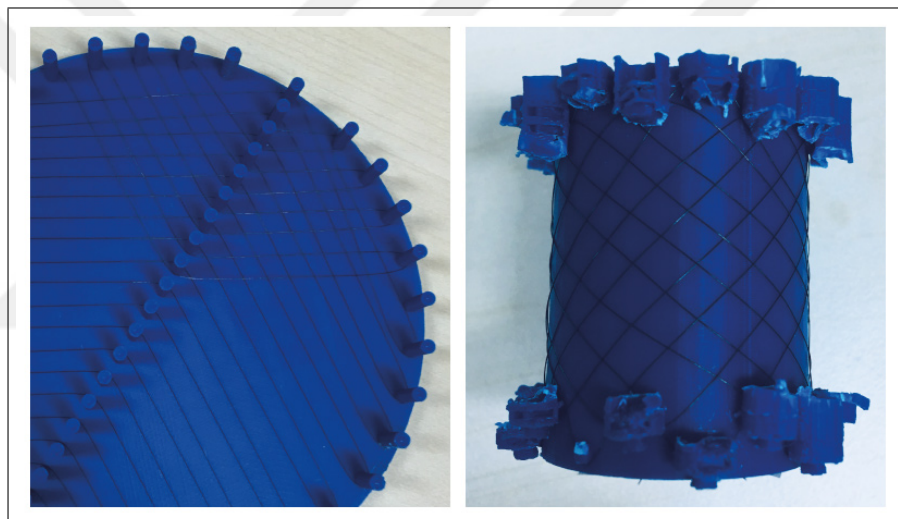


Figure 3.15 Manual braiding trials.

In order to reduce the occluder frame size, further designs were developed using the nitinol wires instead of braided mesh.

The frame shown in Figure 3.16 consists of 6 separately formed 0.009 inches in diameter round nitinol wires (Nitinol Devices & Components, Inc.) around a 2.34 mm diameter ring marker.

In order to increase the surface to volume ratio of the nitinol wires in the design and consequently enhance the adhesion strength with polymer coating, nitinol round wires replaced with 0.004x0.022 inches flat nitinol wires (Fort Wayne Metals Research

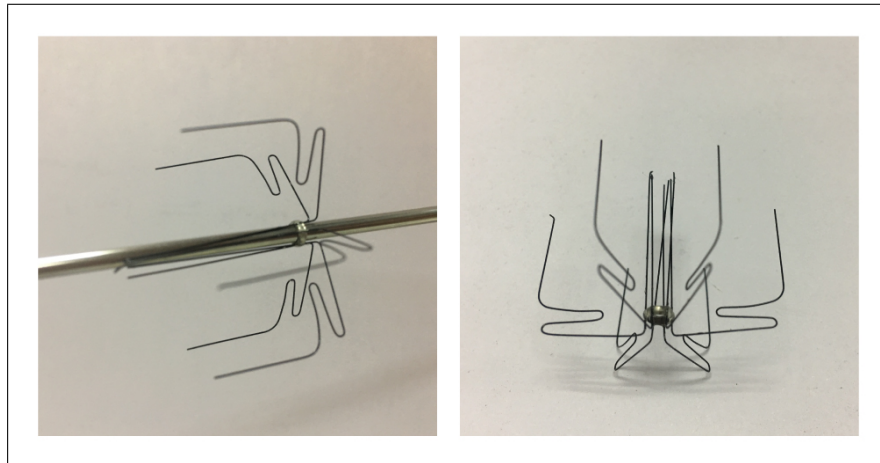


Figure 3.16 Occluder frame with round nitinol wires.

Products Corp.). This also resulted in an overall reduction of the profile of the occluder frame. Round and flat nitinol wires were shaped with the metal mold shown in Figure 3.17.

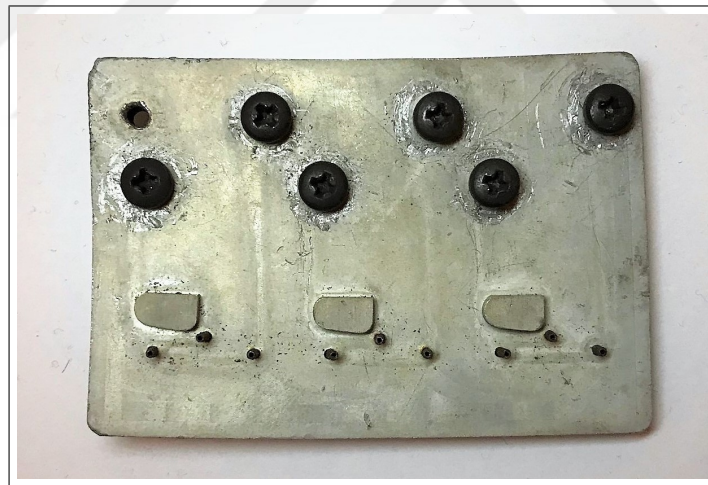


Figure 3.17 The aluminum mold used for shape setting procedure of round and flat nitinol wires with sharp distal ends.

Prepared nitinol wires were formed around the ring marker at a distance of 1.9 mm from each other to form a circular structure using DYMAX Multi-Cure[®] 203A-CTH-F UV curable adhesives and (Omnicure LX 400+) UV curing equipment shown in Figure 3.18.



Figure 3.18 The OmniCure LX 400+ UV light source machine.

The shaped flat wire and formed structure are shown in Figure 3.19.

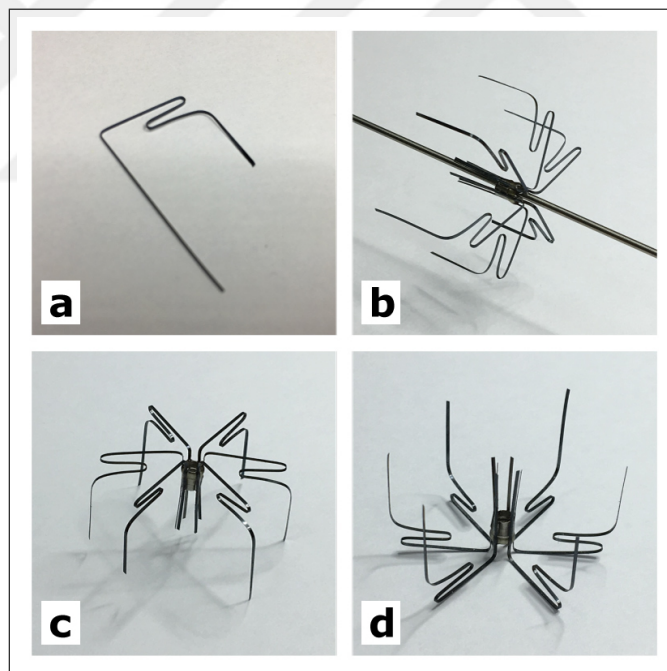


Figure 3.19 (a) Shaped flat nitinol wire. (b, c, d) Occluder frame with flat nitinol wires.

In order to prevent LAA tissue perforation due to sharp distal ends of the nitinol wires, occluder frame design was modified using curved end nitinol wires (in Figure 3.20).



Figure 3.20 Occluder frame with curved end flat nitinol wires.

All occluder prototypes were formed in size of 28 mm. In order to achieve this size, the individual wire dimensions forming the disc-like part of the occluder were shape-set as an average of 12.5 mm in length. However, there were minor deviations due to the manually performed shape-setting procedures.

For the LAA sac volume reduction procedure, the 0.005 inches in diameter nitinol round wire was used to form a 0.18 inches in diameter clover leaf shaped deployable anchor structure. 6-leaf and 3-leaf clover-shaped nitinol anchors are shown in Figure 3.21.

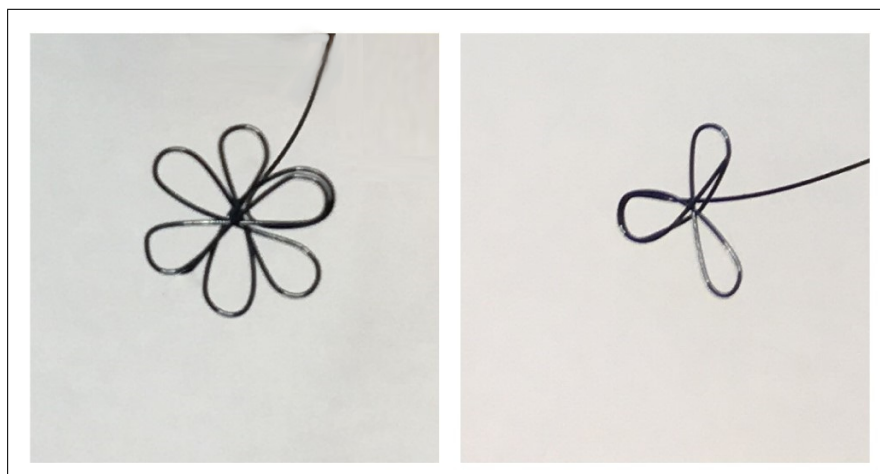


Figure 3.21 6-leaf (left) and 3-leaf (right) clover-shaped distal nitinol anchor trials.

Aluminum mold (shown in Figure 3.22) was utilized for the heat treatment and shape setting process.



Figure 3.22 The aluminum mold used for shape setting procedure of distal anchor structure.

3.1.3 Coating of the Nitinol LAA Occluder Frame

Coating trials were performed simultaneously with occluder frame prototyping. Within the scope of the trials, the focus was primarily on the coating of proximal disc of occluder frame.

Food grade silicone (Mold StarTM 20T) was applied during coating procedure. The components A and B were homogeneously mixed at a ratio of 1:1 and poured in a plastic mold. The occluder frame was placed in the mold and cured for up to 6 hours. Finalized silicone-coated proximal disc of nitinol occluder frame is shown in Figure 3.23.

The weakness of adhesion strength between nitinol and silicone was realized by visual inspection, consequent trials were proceeded with polyurethane as a possible alternative.

In order to coat the proximal end of the occluder using polyurethane, diisocyanate was reacted with the polycarbonate diol. Once the prepolymer was formed, chain extender was added into reaction. Finally, with addition of the crosslinker, a

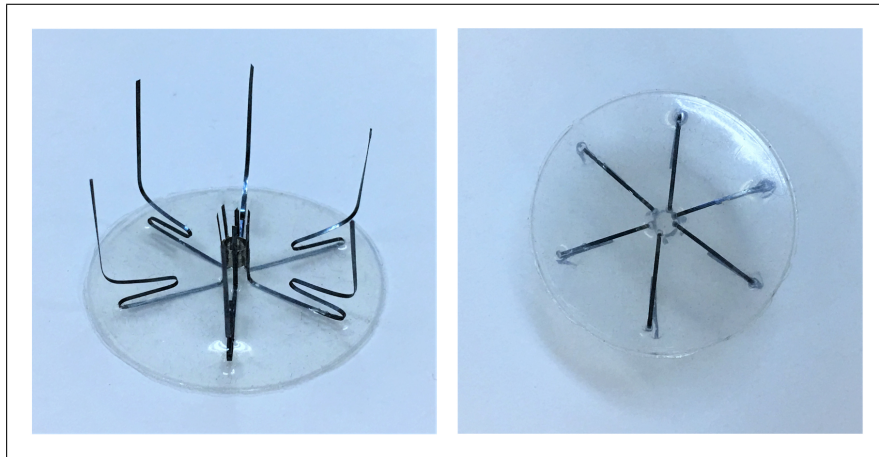


Figure 3.23 Silicone-coated proximal disc of nitinol occluder frame.

homogeneous mixture was obtained and poured into the mold. Occluder frame was placed in the polytetrafluoroethylene (PTFE) mold filled with this solution and cured overnight at 100 °C . Finalized polyurethane-coated proximal disc of nitinol occluder frame is shown in Figure 3.24.

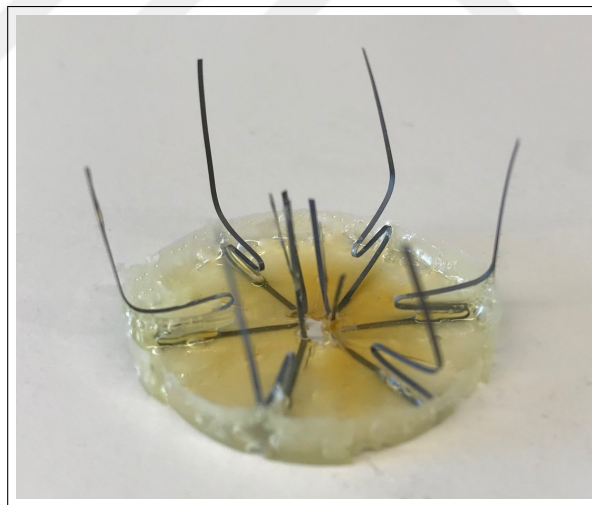


Figure 3.24 Polyurethane-coated proximal disc of nitinol occluder frame.

Since the fully coating of the occluder frame could not be performed due to the polyurethane curing time and properties, the final occluder frame design was coated with silicone (in Figure 3.26) on the PTFE mold (in Figure 3.25) to be used during the sealing tests on the phantom system.

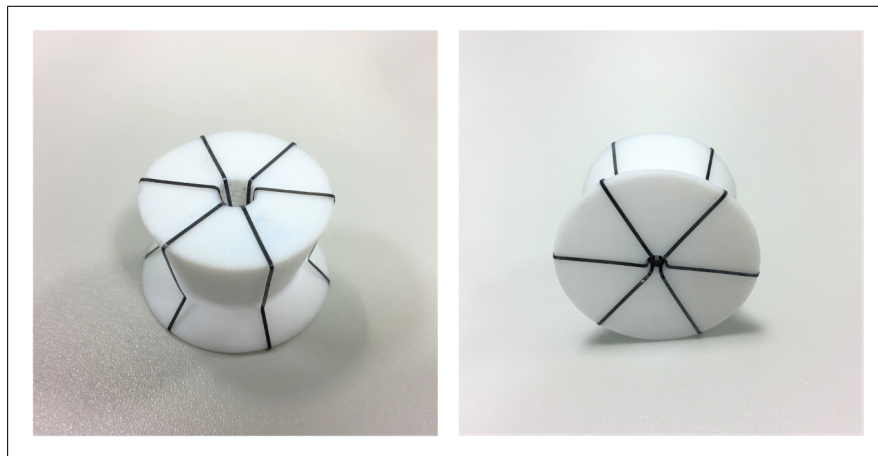


Figure 3.25 PTFE mold designed for fully coating of occluder frame.

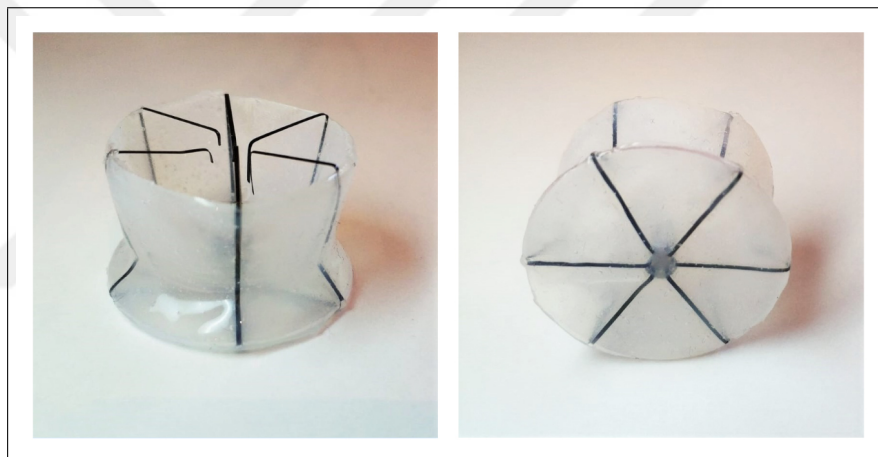


Figure 3.26 Fully silicone-coated nitinol occluder frame.

3.1.4 The Delivery System of the Nitinol LAA Closure Device

Coaxial delivery system was designed to deliver the distal anchor and proximal LAA closure disc independently.

The coaxial device delivery and deployment system consists of a delivery catheter of occluder frame (transparent outer catheter), a fixed catheter (middle catheter), a delivery catheter of distal anchor (inner catheter) (shown in Figure 3.27), and a control handle.

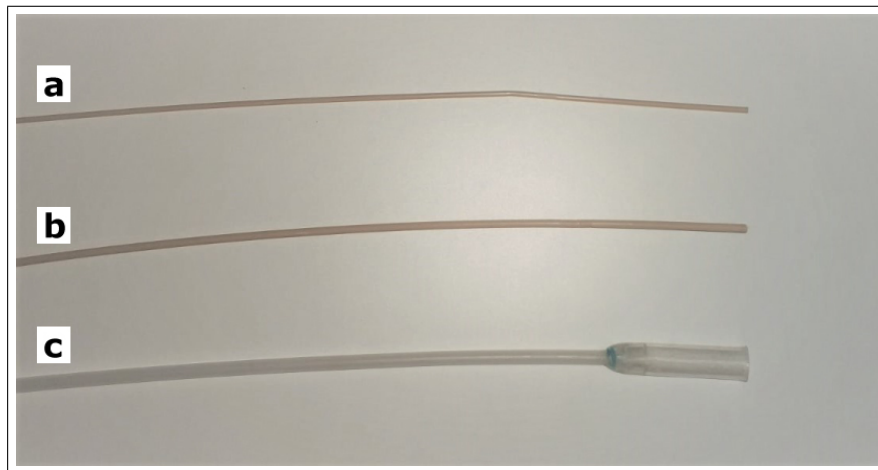


Figure 3.27 (a) Inner delivery catheter, (b) Middle fixed catheter, (c) Outer delivery catheter.

The design of the control handle is illustrated in Figure 3.28.

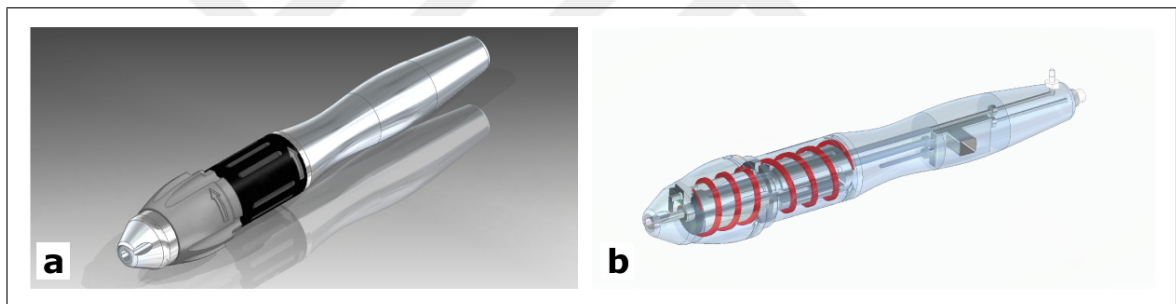


Figure 3.28 (a) Illustration of external view of the control handle, (b) Illustration of internal view of the control handle.

The control handle was prototyped using five fixed components, two rotatable deployment knobs and mandrels (shown in Figure 3.29).

The outer catheter was designed to deliver the self-expanding nitinol occluder frame. The proximal end of the catheter is 0.1 inches in inner diameter, while the distal end is 0.3 inches in inner diameter to house the occluder (shown in Figure 3.30). Proximal end of the outer catheter was attached to proximal deployment knob.

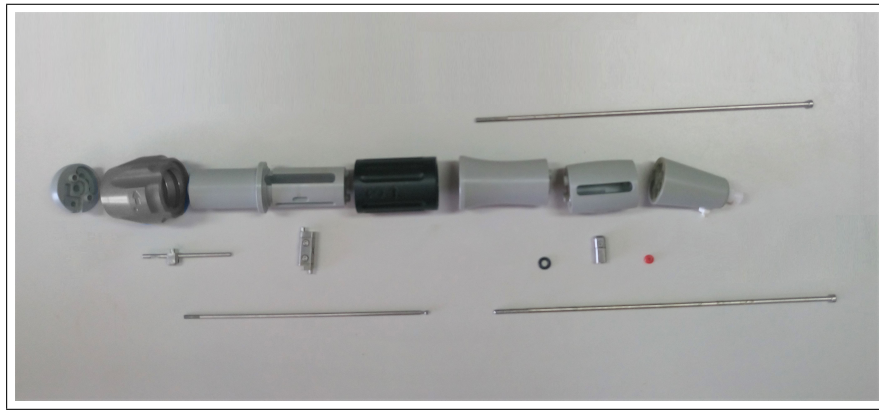


Figure 3.29 The components of the control handle.

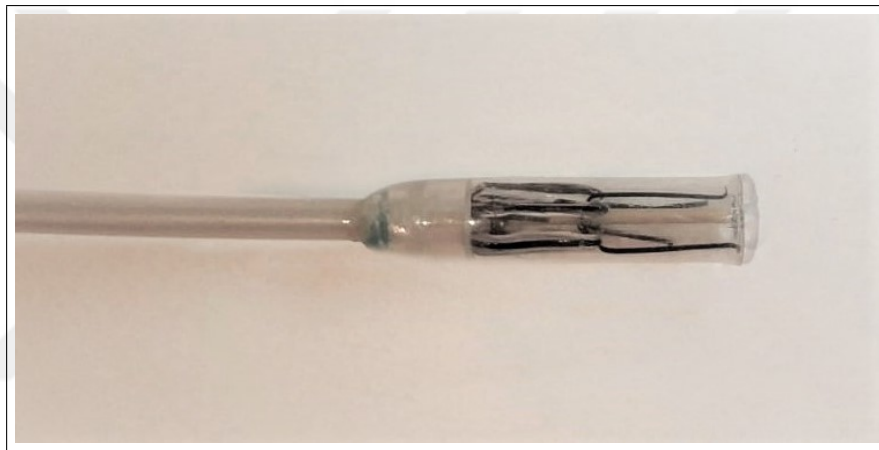


Figure 3.30 Nitinol occluder frame encapsulated in the distal end of the outer catheter.

The middle fixed catheter was chosen with 0.08 inches in outer and 0.06 inches in inner diameter in order to prevent occluder frame movement during deployment procedure.

The inner catheter was preferred 0.05 inches in outer and 0.03 inches in inner diameter to be movable within the middle catheter and advance the distal anchor through LAA tissue. It was attached to distal deployment knob.

The nitinol occluder components on the coaxial delivery catheter system were demonstrated in Figure 3.31.

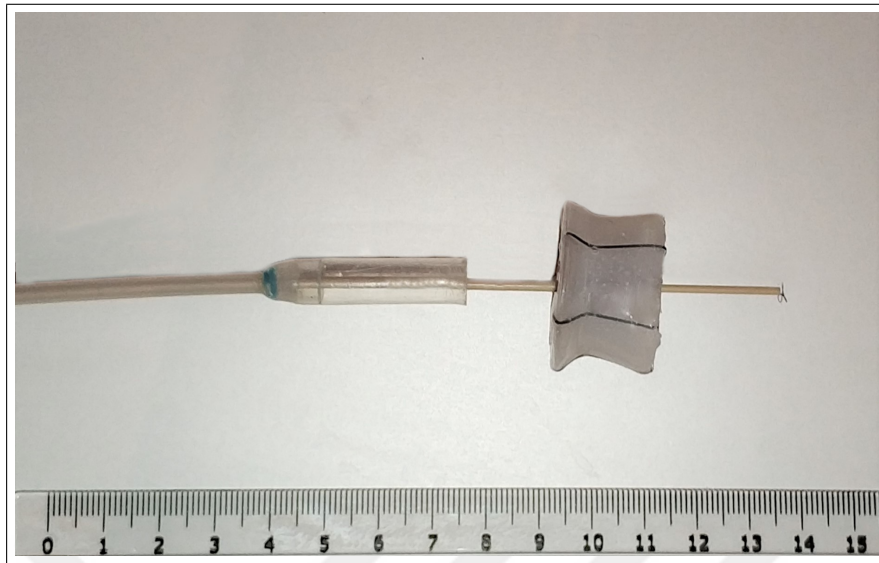


Figure 3.31 The demonstration of deployed occluder components on the delivery catheters.

The prototyped coaxial delivery system is shown in Figure 3.32

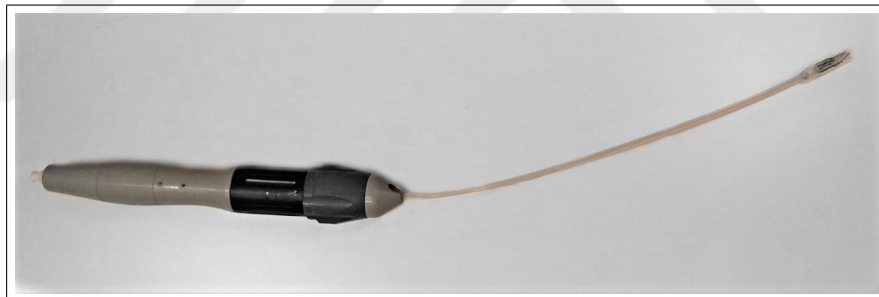


Figure 3.32 The complete delivery system.

3.1.5 In Vitro LAA Phantom

In order to evaluate the prototyped nitinol occluder frame, a silicone-based LAA phantom was fabricated to simulate the procedure. The phantom system consists of three sub-systems: anatomical heart model with LAA, peristaltic pump, pressure sensors and controller circuit. The overall system is depicted in Figure 3.33 and the complete phantom system is shown in Figure 3.34.

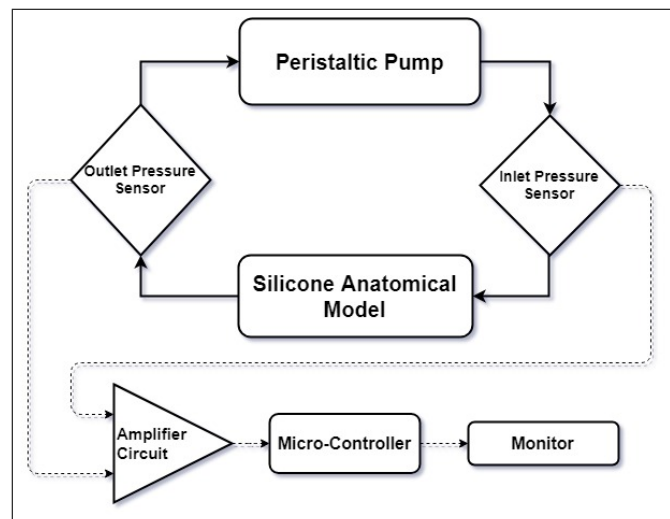


Figure 3.33 Functional block diagram of the components of the heart phantom.

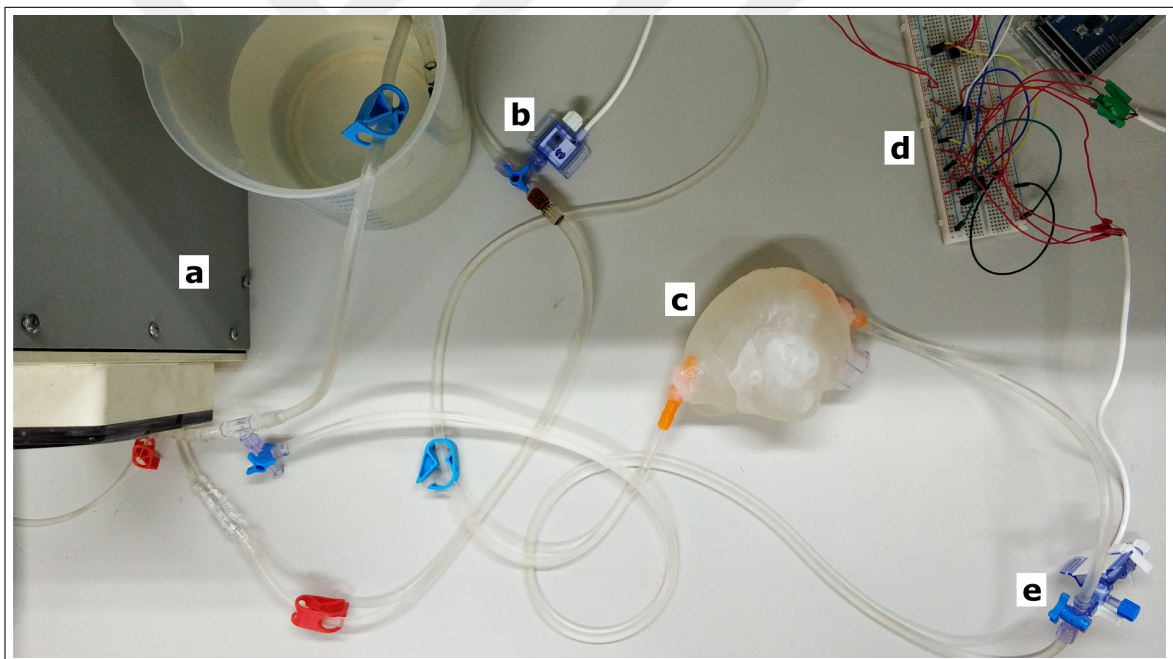


Figure 3.34 The overall picture of the in vitro LAA phantom: (a) Peristaltic pump, (b,e) Pressure sensors, (c) Silicone left atrium heart model, (d) Amplifier circuit and micro-controller.

The silicone based left atrium heart model at the phantom was formed by coating silicone on top of the 3D printed heart model (shown in Figure 3.35).

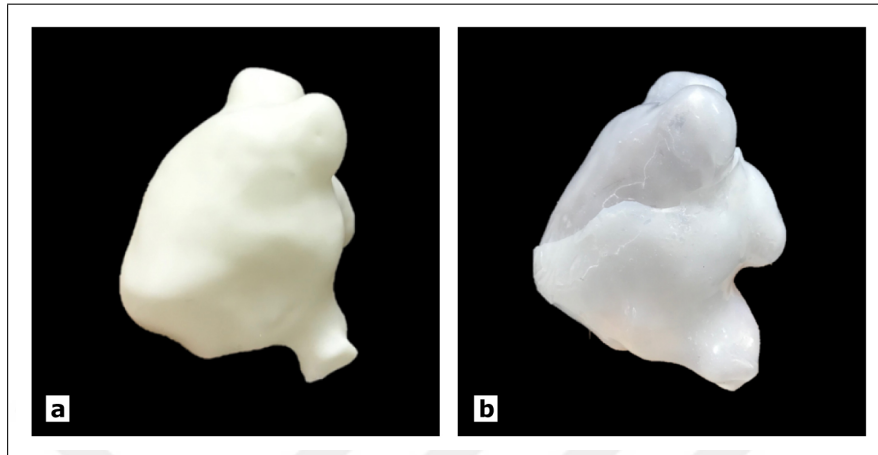


Figure 3.35 (a) 3D-printed heart model, (b) Silicone anatomical model.

Since the primary goal was to mimic the appendage in the left atrium, blood flow cycles between the pump and the heart model were simulated. During the simulation, inlet and outlet pressure values were maintained between 10-30 mmHg which is average left atrium pressure. As a medium compatible with silicone, water was used to simulate blood throughout the system.

Two pressure sensors were attached to the ports positioned at the inlet and outlet of anatomical heart model to regulate and maintain the intended pressure values. The sensors were connected to a computer through an Arduino Mega configuration to monitor the real-time pressure values.

This phantom was intended to provide a realistic mechanical model for occlusion procedure of LAA ostium.

3.2 Testing Procedure

3.2.1 Tensile Test

Tensile testing is a basic materials science test where the sample is load uniaxially until failure. The results from the tensile test are used for material selection, quality control and predicting the material behaviour under the forces.

In order to assess mechanical properties of silicone and polyurethane materials, tensile tests were applied to 4 silicone and 4 polyurethane dog-bone shaped (illustrated in Figure 3.36) specimens with 2mm thickness. The dimensions of specimens and tensile testing speed of 25 mm/min were determined according to ISO-527 standard [55].

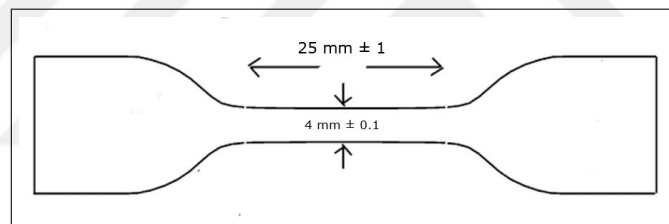


Figure 3.36 Dimensions of the dog-bone tensile test specimen.

Tensile tests were performed using a tensile testing unit (Zwick Roell zwickiLine) (Figure 3.37) fitted with a 2.5 kN load cell.



Figure 3.37 Tensile test setup (Zwick Roell zwickiLine).

3.2.2 Shear Test

Shear test was used as mechanical assessment procedure to measure the adhesion strength. It was used to compare the bond quality between silicone with nitinol and polyurethane with nitinol. This test was also carried out using the material testing device.

Silicone- and polyurethane coated occluder frames were cut into pieces (in Figure 3.38) with a nitinol wire within the middle of each piece. Shear tests were performed on these specimens.

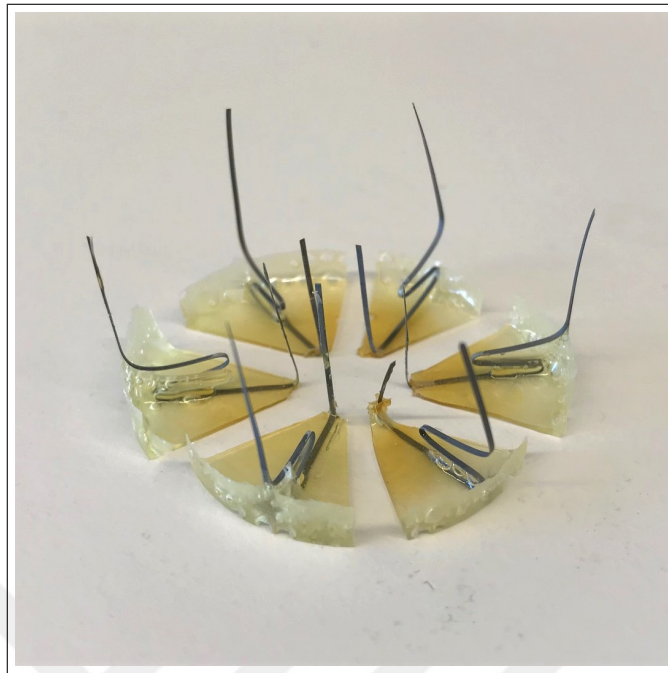


Figure 3.38 Polyurethane coated nitinol specimens.

3.2.3 Sealing Test

In order to evaluate the sealing quality of LAA ostium using prototyped nitinol occluder frame, a sealing test was performed on the designed phantom.

To perform the sealing test, thrombus-like structures were filled into the LAA model and the silicone-coated occluder frame was placed into the same model (in Figure 3.39).

15-minute period of circulation was performed under the defined LA pressure values (10-30 mmHg) after the LAA closure device deployment and visual inspection was performed to evaluate any clot migration.

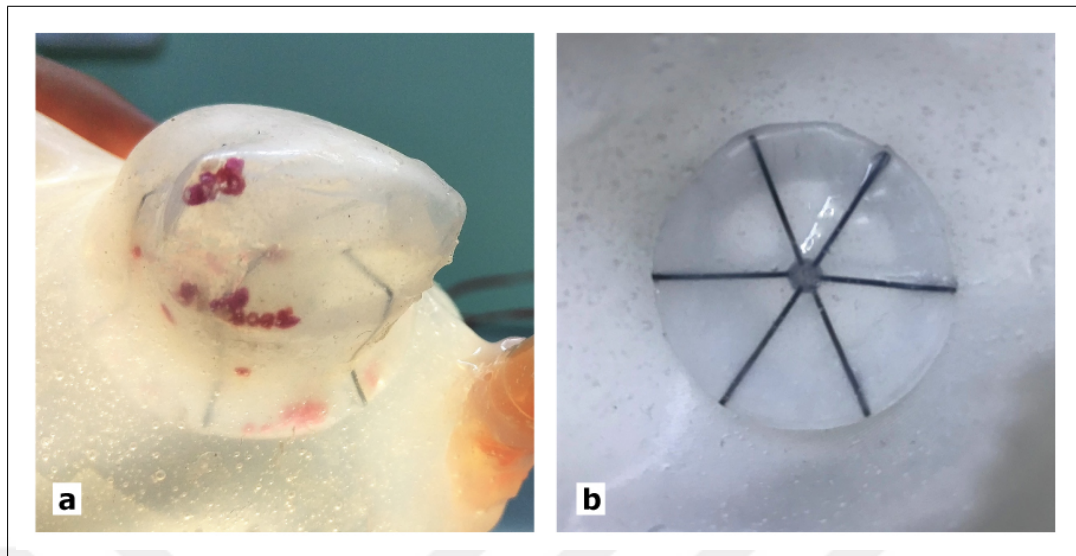


Figure 3.39 (a) Encapsulated thrombus-like structures in LAA model (b) Silicone-coated occluder appearance after fitting into LAA ostium.

4. RESULTS

The tensile test results obtained from the material testing device are shown in Figure 4.1

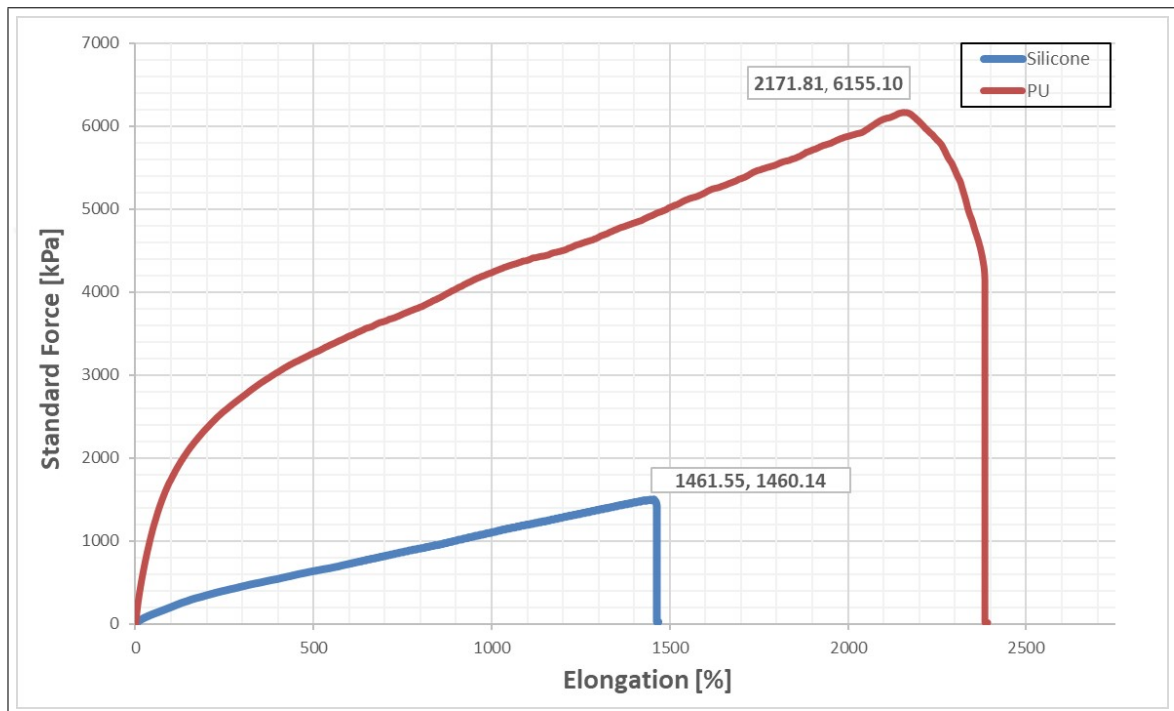


Figure 4.1 The tensile test results.

In Figure 4.1, the standard force vs. elongation dependences measured for polyurethane and silicone specimens are plotted. The silicone and polyurethane specimen test results, corresponding to the mean values of four tests are represented by blue and red curves, respectively. The uppermost point of the blue curve (1460.14 kPa) indicates the breaking point of silicone, while uppermost point of the red curve (6155.10 kPa) was caused by polyurethane specimen slippage from jaw.

The performed shear test results to assess the adhesion strength between silicone with nitinol and polyurethane with nitinol are shown in Figure 4.2.

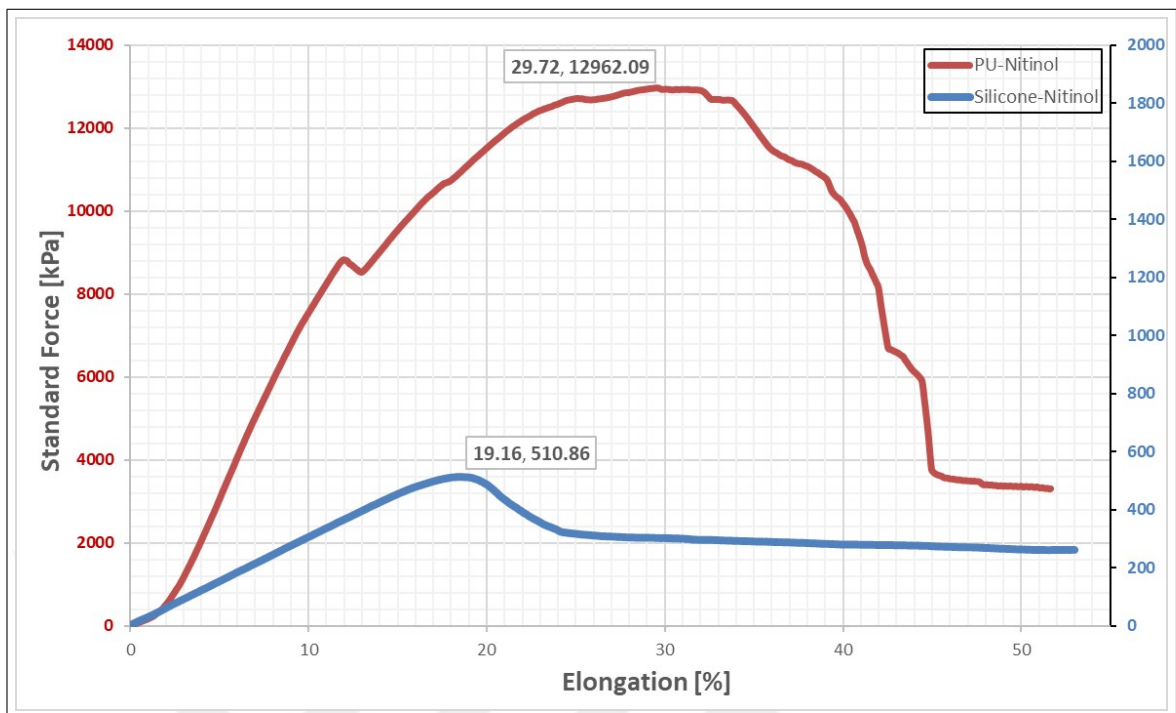


Figure 4.2 Shear test results.

The peak point of the blue curve (510.86 kPa) indicates slippage-point of nitinol from the silicone coating. Images obtained during the process are shown in Figure 4.3.

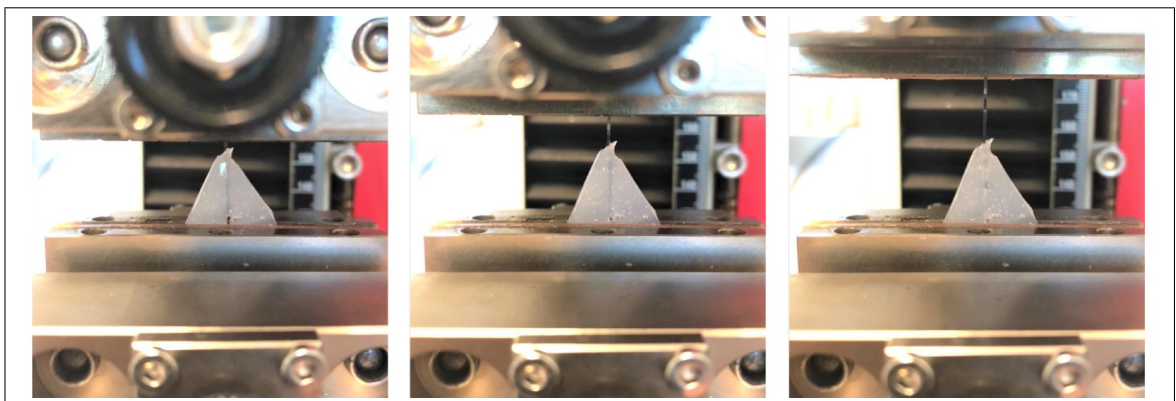


Figure 4.3 Images obtained during shear test procedure of silicone-coated nitinol specimen at 5, 20 and 40 seconds, respectively.

The uppermost point (6155.10 kPa) of the red curve was caused by polyurethane coating breakage due to air-bubble forms in coating. Images obtained during the process are shown in Figure 4.4.

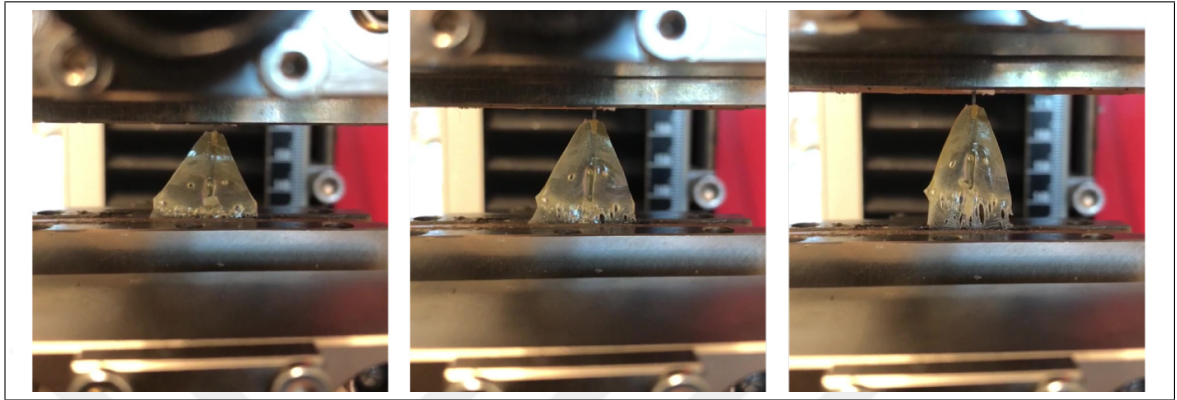


Figure 4.4 Images obtained during shear test procedure of polyurethane-coated nitinol specimen at 5, 20 and 40 seconds, respectively.

Sealing tests of prototyped silicone-coated occluder frame placed into the LAA anatomical model were performed using the phantom system while monitoring real-time pressure values (shown in Figure 4.5). The pressure measurements acquired during the procedure in this experiment were observed between 12 and 30 mmHg.

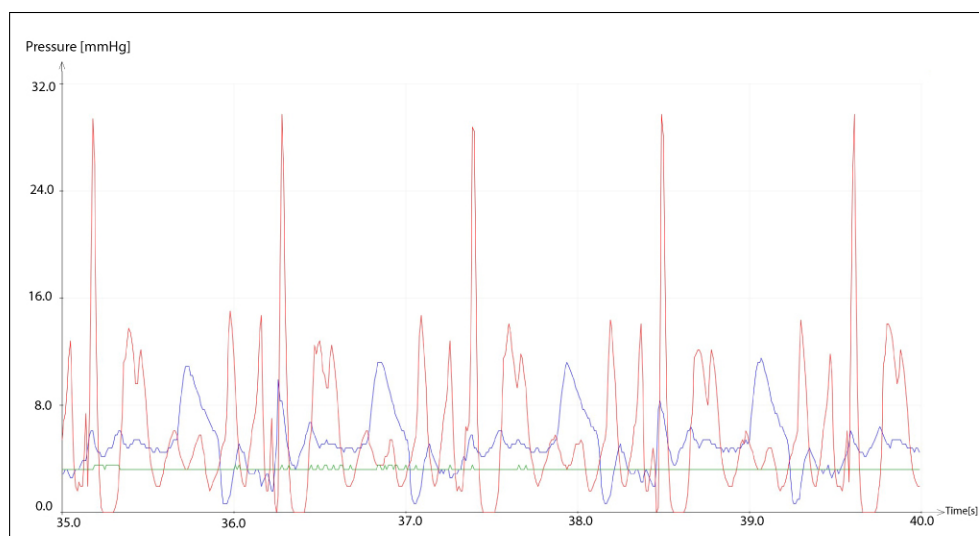


Figure 4.5 Real-time pressure values of sealing test procedure.

Thrombus-like structures were not observed in the system outside the LAA during 15-minute period of circulation (shown in Figure 4.6).

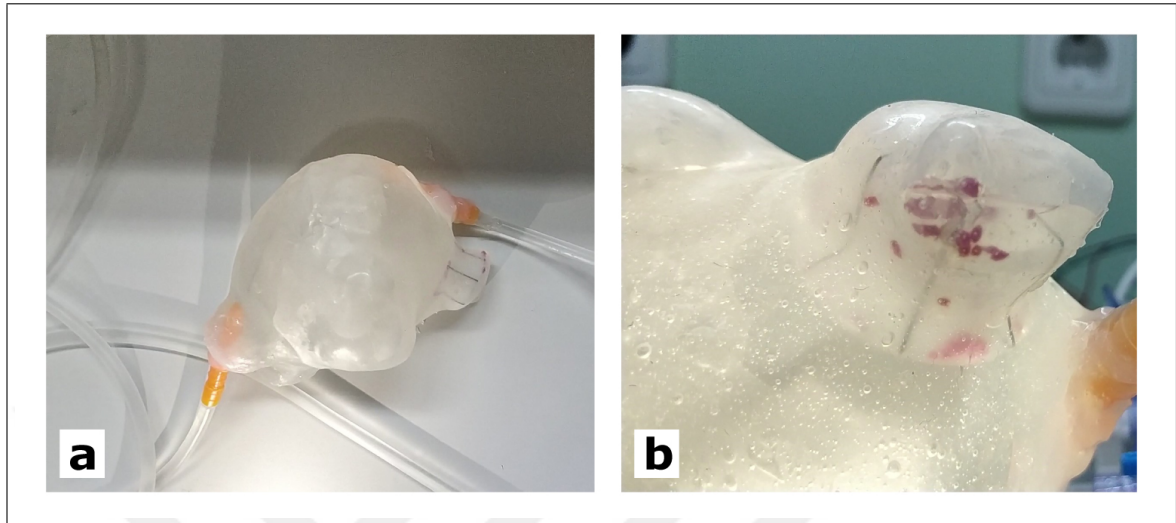


Figure 4.6 Images of (a) the complete anatomical heart model and (b) the LAA part of the anatomical model obtained at the end of the 15 minutes sealing test procedure.

Distal nitinol anchor was used to reduce the LAA sac volume, consequently the movement of thrombus-like structures into the occluder was observed (Figure 4.7).

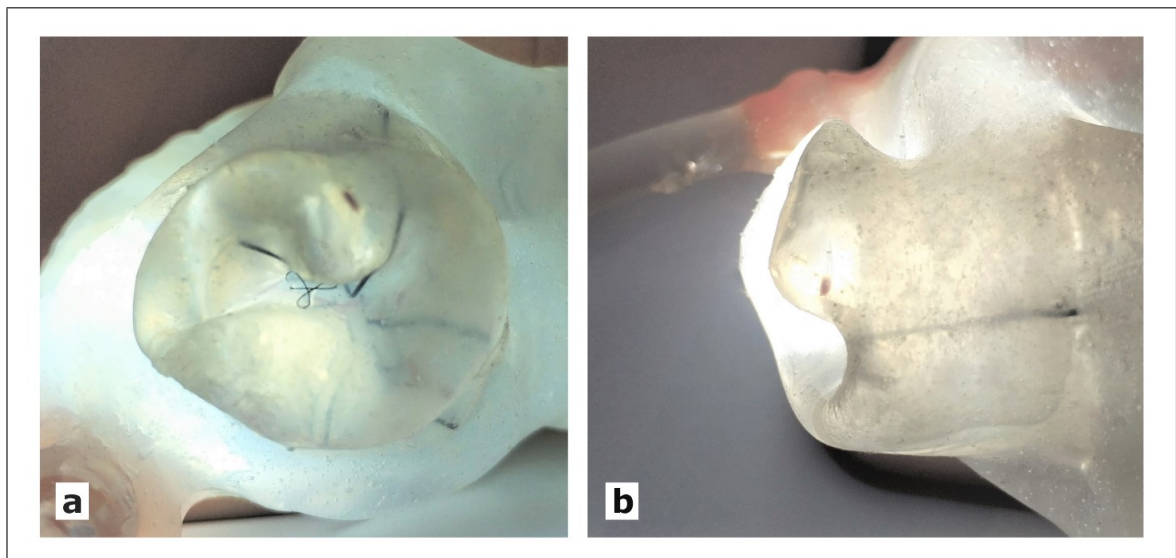


Figure 4.7 Images of front (a) and side (b) views of the reduced LAA sac by volume.

5. DISCUSSION

This thesis study aims to develop a novel Left Atrial Appendage occluder device design with improved performance in comparison to the conventional solutions.

In order to design a novel occluder, morphological structure of the sample LAA model was 3D printed and modelled using silicone. The device design based on prepared models demonstrates an approach to decrease the LAA sac volume while sealing the ostium. Even though mesh structured occluders are commercially available, a novel method for anchoring the distal end of the LAA sac during occlusion procedure was demonstrated.

Once the LAA occluder design was finalized, the device parts were started to be prototyped. Different geometries of occluder frame in defined sizes were prototyped with designed aluminum molds and implemented on 3D silicone models. The final occluder frame design introduces a successful sealing as well as a locking mechanism to prevent the migration of the occluder in LAA neck. In this design, the distal ends of the nitinol wires are curved inwards to prevent a perforation-induced adverse event during the LAA sac volume reduction procedure which is the most important procedural design novelty that differentiate our design from commercial products on the market. Additionally, it has been demonstrated that using flat nitinol wire and applying sand blasting enhance the adhesion strength with coating material in the final design.

In order to ensure that the final occluder frame design provides the effective sealing of LAA ostium, and also prevents device associated thrombus formation, coating trials were conducted using silicone and polyurethane. However, the fully coated occluder frame could only be prepared with silicone due to the physical properties of the occluder as well as curing time and chemical properties of polyurethane. The proposed silicone-coated occluder design performance was evaluated via an in vitro test mimicking the environment and morphology of the LAA using an in-house built liq-

uid filled phantom under defined pressure conditions. Thrombus-like structures were not observed outside the LAA. The phantom study results with the novel LAA occluder frame prototype have demonstrated that the fully coated occluder frame can successfully seal the LAA ostium.

As a part of this study, distal anchor component of the occluder design was prototyped in order to reduce the LAA sac volume and to prevent new thrombus formation.

Although silicone-coated occluder frame study is a proof-of-concept, silicone as a coating material should be replaced by a more functional, durable and flexible material for further studies. Polyurethane was considered as a possible option for coating compared with silicone via mechanical assessments. According to the tensile test results polyurethane has more than 4-times greater tensile strength than silicone due to its cross-linking ability and chain flexibility. Additionally, shear test results showed that adhesion quality between polyurethane and nitinol is over 26 times greater than silicone-nitinol adhesion. Visual evaluation of the mechanical tests suggest that the silicone and nitinol adhesion was formed via physical bonds while polyurethane-nitinol adhesion was formed mostly chemical.

A custom percutaneous based coaxial delivery system was designed and prototyped for delivery and deployment of occluder into LAA. The delivery system was designed with using the outer catheter to house a polyurethane-coated occluder. However, the trials were conducted with an uncoated occluder frame due to the fact that the occluder coated with silicone, which was a thicker material, could not placed into the outer catheter.

6. CONCLUSION AND FUTURE WORKS

The occlusion of the left atrial appendage (LAA) through interventional procedure is a promising alternative to continual oral anticoagulation therapy in patients with non-valvular atrial fibrillation. The current LAA occlusion options include significant complications such as occluder embolism and tissue perforation leading to cardiac deaths. Therefore, this study has focused on the development of a novel LAA occlusion device design. This device design demonstrated a new procedure to prevent further thrombus formation after implantation by anchoring the distal end of the LAA.

Results of this study shows that the novel design of the occluder frame component is a promising candidate for sealing the LAA ostium in order to prevent thrombus leakage and occluder migration in comparison to commercial products.

Further prospective studies should be conducted to develop new nitinol occluder frame design in order to provide better sealing and to ensure preventing occluder embolization.

In its final form, silicone coating thickness of the occluder frame should be reduced to fit it into smaller catheter in diameter to deliver it percutaneously. Polyurethane was chosen as a possible coating material due to its adhesion quality. However, different manufacturing techniques can be applied instead of dipping method to form fully-coated nitinol occluder frame using polyurethane.

Further studies should also include distal anchor force tests to assess the effect on distal end of the LAA during sac volume reduction procedure. In addition, hollow suture locking mechanism with nitinol tines should be prototyped to lock the distal nitinol anchor to the nitinol occluder frame.

Further evaluation of the coaxial catheter delivery system should be carried out with a polyurethane-coated nitinol occluder frame and hollow suture mechanism. Modifications of the delivery system should be applied to keep the maximum profile smaller.

Future research should include in-vivo studies in order to assess endothelialization, thrombus formation on occluder and long-term stability.



REFERENCES

1. Chung, M. K., and M. W. Rich, "Introduction to the cardiovascular system," *Alcohol Research*, Vol. 14, no. 4, p. 269, 1990.
2. Iaizzo, P. A., *Handbook of Cardiac Anatomy, Physiology, and Devices*, Springer Science & Business Media, 2009.
3. Scanlon, V. C., and T. Sanders, *Essentials of Anatomy and Physiology*, FA Davis, 2018.
4. Goldberger, A. L., Z. D. Goldberger, and A. Shvilkin, *Clinical Electrocardiography: A Simplified Approach E-Book: A Simplified Approach*, Elsevier Health Sciences, 2017.
5. Saw, J., S. Kar, and M. J. Price, *Left Atrial Appendage Closure*, Springer, 2015.
6. Bosi, G. M., A. Cook, R. Rai, L. J. Menezes, S. Schievano, R. Torii, and G. B. Burriesci, "Computational fluid dynamic analysis of the left atrial appendage to predict thrombosis risk," *Frontiers in Cardiovascular Medicine*, Vol. 5, p. 34, 2018.
7. Suwalski, P., A. Witkowska, D. Drobiński, J. Rozbicka, S. Sypuła, I. Liszka, R. Smoczyński, J. Staromłyński, I. Walecka, and D. Kosior, "Stand-alone totally thoracoscopic left atrial appendage exclusion using a novel clipping system in patients with high risk of stroke—initial experience and literature review," *Kardiologia i Torakochirurgia Polska= Polish Journal of Cardio-thoracic Surgery*, Vol. 12, no. 4, p. 298, 2015.
8. Philippsen, L. P., E. C. Weisberger, T. S. Whiteman, and J. L. Schmidt, "Endoscopic stapled diverticulotomy: treatment of choice for zenker's diverticulum," *The Laryngoscope*, Vol. 110, no. 8, pp. 1283–1286, 2000.
9. Ohtsuka, T., M. Ninomiya, T. Nonaka, M. Hisagi, T. Ota, and T. Mizutani, "Thoracoscopic stand-alone left atrial appendectomy for thromboembolism prevention in nonvalvular atrial fibrillation," *Journal of the American College of Cardiology*, Vol. 62, no. 2, pp. 103–107, 2013.
10. Ostermayer, S. H., M. Reisman, P. H. Kramer, R. V. Matthews, W. A. Gray, P. C. Block, H. Omran, A. L. Bartorelli, P. Della Bella, C. Di Mario, *et al.*, "Percutaneous left atrial appendage transcatheter occlusion (plaat system) to prevent stroke in high-risk patients with non-rheumatic atrial fibrillation: results from the international multi-center feasibility trials," *Journal of the American College of Cardiology*, Vol. 46, no. 1, pp. 9–14, 2005.
11. Saw, J., "Amplatz cardiac plug and amulet," in *Left Atrial Appendage Closure*, pp. 181–193, Springer, 2016.
12. Ridder, S. D., M.-J. Suttorp, S. M. Ernst, J. A. Six1, H. F. Mannaerts, O. Kamp, T. H. Plokker, and W. Jaarsma1, "Percutaneous transcatheter closure of atrial septal defects: initial single-centre experience and follow-up results. initial experience with three-dimensional echocardiography.," *Acta Cardiologica*, Vol. 60, no. 2, pp. 171–178, 2005.
13. Luis, S. A., D. Roper, A. Incani, K. Poon, H. Haqqani, and D. L. Walters, "Non-pharmacological therapy for atrial fibrillation: managing the left atrial appendage," *Cardiology Research and Practice*, Vol. 2012, 2012.

14. Şahin, D. Y., M. Koç, H. Çakır, O. Z. Arık, Z. Elbasan, and M. Çaylı, “A silent and late embolization of atrial septal defect occluder device into the right pulmonary artery: a case report,” *Korean Circulation Journal*, Vol. 42, no. 11, pp. 781–783, 2012.
15. Pavlicevic, J., M. Spirkov, O. Bera, M. Jovicic, K. Meszaros Szecsenyi, and J. Budinski-Simendic, “Macedonian bentonte,” 11 2016.
16. Price, M. J., D. N. Gibson, S. J. Yakubov, J. C. Schultz, L. Di Biase, A. Natale, J. D. Burkhardt, A. Pershad, T. J. Byrne, B. Gidney, *et al.*, “Early safety and efficacy of percutaneous left atrial appendage suture ligation: results from the us transcatheter laa ligation consortium,” *Journal of the American College of Cardiology*, Vol. 64, no. 6, pp. 565–572, 2014.
17. Opie, L. H., *Heart Physiology: From Cell to Circulation*, Lippincott Williams & Wilkins, 2004.
18. Podrid, P. J., and P. R. Kowey, *Cardiac Arrhythmia: Mechanisms, Diagnosis, and Management*, Lippincott Williams & Wilkins, 2001.
19. Shah, S. R., K. Park, and R. Alweis, “Long qt syndrome: a comprehensive review of the literature and current evidence,” *Current Problems in Cardiology*, Vol. 44, no. 3, pp. 92–106, 2019.
20. Dowd, F., “Ventricular fibrillation and flutter,” *Reference Module in Biomedical Sciences*, 2014.
21. Ganz, L. I., and P. L. Friedman, “Supraventricular tachycardia,” *New England Journal of Medicine*, Vol. 332, no. 3, pp. 162–173, 1995.
22. Cosío, F. G., “Atrial flutter, typical and atypical: a review,” *Arrhythmia & Electrophysiology Review*, Vol. 6, no. 2, p. 55, 2017.
23. Mozaffarian, D., E. J. Benjamin, A. S. Go, D. K. Arnett, M. J. Blaha, M. Cushman, S. R. Das, S. de Ferranti, J. P. Després, H. J. Fullerton, *et al.*, “Heart disease and stroke statistics-2016 update a report from the american heart association,” *Circulation*, Vol. 133, no. 4, pp. e38–e48, 2016.
24. Kirchhof, P., A. Auricchio, J. Bax, H. Crijns, J. Camm, H.-C. Diener, A. Goette, G. Hindricks, S. Hohnloser, L. Kappenberger, *et al.*, “Outcome parameters for trials in atrial fibrillation: executive summary: Recommendations from a consensus conference organized by the german atrial fibrillation competence network (afnet) and the european heart rhythm association (ehra),” *European Heart Journal*, Vol. 28, no. 22, pp. 2803–2817, 2007.
25. Wolf, P. A., R. D. Abbott, and W. B. Kannel, “Atrial fibrillation as an independent risk factor for stroke: the framingham study.,” *Stroke*, Vol. 22, no. 8, pp. 983–988, 1991.
26. Benjamin, E. J., D. Levy, R. B. D’Agostino, A. J. Belanger, and P. A. Wolf, “754-3 impact of atrial fibrillation on the risk of death: The framingham study,” *Journal of the American College of Cardiology*, Vol. 25, no. 2 Supplement 1, p. 230A, 1995.
27. Yu, C.-M., A. A. Khattab, S. C. Bertog, A. P. Lee, J. S. Kwong, H. Sievert, and B. Meier, “Mechanical antithrombotic intervention by laa occlusion in atrial fibrillation,” *Nature Reviews Cardiology*, Vol. 10, no. 12, p. 707, 2013.

28. Ernst, G., C. Stöllberger, and J. Finsterer, "Determination of left atrial appendage morphology," *Circulation*, Vol. 98, pp. 2355–2355, 1998.
29. Baer, H., D. Mereles, E. Grünig, and H. Kuecherer, "Exaggerated pectinate muscles mimicking multiple left atrial appendage thrombi," *European Journal of Echocardiography*, Vol. 2, no. 2, pp. 131–131, 2001.
30. Beinart, R., E. K. Heist, J. B. Newell, G. Holmvang, J. N. Ruskin, and M. Mansour, "Left atrial appendage dimensions predict the risk of stroke/tia in patients with atrial fibrillation," *Journal of Cardiovascular Electrophysiology*, Vol. 22, no. 1, pp. 10–15, 2011.
31. Robinson, S. S., S. Alaie, H. Sidoti, J. Auge, L. Baskaran, K. Avilés-Fernández, S. D. Hollenberg, R. F. Shepherd, J. K. Min, S. N. Dunham, *et al.*, "Patient-specific design of a soft occluder for the left atrial appendage," *Nature Biomedical Engineering*, Vol. 2, no. 1, p. 8, 2018.
32. Johnson, W. D., A. Ganjoo, C. D. Stone, R. C. Srivivas, and M. Howard, "The left atrial appendage: our most lethal human attachment! surgical implications," *European Journal of Cardio-Thoracic Surgery*, Vol. 17, no. 6, pp. 718–722, 2000.
33. Aryana, A., S. K. Singh, S. M. Singh, P. G. O'Neill, M. R. Bowers, S. L. Allen, S. L. Lewandowski, E. C. Vierra, and A. d'Avila, "Association between incomplete surgical ligation of left atrial appendage and stroke and systemic embolization," *Heart Rhythm*, Vol. 12, no. 7, pp. 1431–1437, 2015.
34. Gillinov, A. M., G. Pettersson, and D. M. Cosgrove, "Stapled excision of the left atrial appendage," *The Journal of Thoracic and Cardiovascular surgery*, Vol. 129, no. 3, pp. 679–680, 2005.
35. Incorporated, A., *PDP90A Position Sensing Detector User Guide*. AtriCure Incorporated.
36. Estes III, N. M., and A. L. Waldo, *Atrial Fibrillation: A Multidisciplinary Approach to Improving Patient Outcomes*, Vol. 4, Cardiotext Publishing, 2015.
37. Onalan, O., and E. Crystal, "Left atrial appendage exclusion for stroke prevention in patients with nonrheumatic atrial fibrillation," *Stroke*, Vol. 38, no. 2, pp. 624–630, 2007.
38. Pacha, H. M., Y. Al-khadra, M. Soud, F. Darmoch, A. M. Pacha, and M. C. Alraies, "Percutaneous devices for left atrial appendage occlusion: A contemporary review," *World Journal of Cardiology*, Vol. 11, no. 2, p. 57, 2019.
39. Bradley, D. J., and W.-K. Shen, "Atrioventricular junction ablation combined with either right ventricular pacing or cardiac resynchronization therapy for atrial fibrillation: the need for large-scale randomized trials," *Heart Rhythm*, Vol. 4, no. 2, pp. 224–232, 2007.
40. Kanmanthareddy, A., Y. Reddy, J. Pillarisetti, V. Swarup, and D. Lakkireddy, "Laa closure with the watchman device," *Cardiac Interventions Today*, Vol. 5, pp. 35–40, 2013.
41. Safavi-Naeini, P., M. Razavi, M. Saeed, A. Rasekh, and A. Massumi, "A review of the lariat suture delivery device for left atrial appendage closure," *The Journal of Tehran University Heart Center*, Vol. 10, no. 2, p. 69, 2015.

42. Sarcon, A., D. Roy, D. Laughrun, M. Huntsinger, J. Schwartz, J. Sohn, and R. N. Doshi, "Left atrial appendage occlusion complicated by appendage perforation rescued by device deployment," *Journal of Investigative Medicine High Impact Case Reports*, Vol. 6, pp. 1–4, 2018.
43. Food, U., D. Administration, *et al.*, "Design control guidance for medical device manufacturers," *Center for Devices and Radiological Health*, 1997.
44. Gilman, B. L., J. E. Brewer, and M. W. Kroll, "Medical device design process," in *2009 Annual International Conference of the IEEE Engineering in Medicine and Biology Society*, pp. 5609–5612, IEEE, 2009.
45. Panescu, D., "Medical device development," in *2009 Annual International Conference of the IEEE Engineering in Medicine and Biology Society*, pp. 5591–5594, IEEE, 2009.
46. Carey, J. P., *Handbook of Advances in Braided Composite Materials: Theory, Production, Testing and Applications*, Woodhead Publishing, 2016.
47. Aibibu, D., M. Hild, and C. Cherif, "An overview of braiding structure in medical textile: fiber-based implants and tissue engineering," in *Advances in Braiding Technology*, pp. 171–190, Elsevier, 2016.
48. Steeger USA Inc. Company, *K80 Series Horizontal and Vertical Style Braiding Systems*.
49. Corporation, M., *Introduction to Nitinol*. Memry a SAES Group Company, Bethel, CT 06801, 1 ed., 2017. An optional note.
50. Szycher, M., "Polyurethanes: Medical applications," in *Encyclopedia of Biomedical Polymers and Polymeric Biomaterials, 11 Volume Set*, pp. 6647–6670, CRC Press, 2015.
51. Szycher, M., "Polyurethanes: Biodurable," in *Encyclopedia of Biomedical Polymers and Polymeric Biomaterials, 11 Volume Set*, pp. 6630–6646, CRC Press, 2015.
52. Mukherjee, D., E. Bates, M. Roffi, and D. Moliterno, *Cardiovascular Catheterization and Intervention: A Textbook of Coronary, Peripheral, and Structural Heart Disease*, CRC Press, 2010.
53. Stoeckel, D., A. Pelton, and T. Duerig, "Self-expanding nitinol stents: material and design considerations," *European Radiology*, Vol. 14, no. 2, pp. 292–301, 2004.
54. Braune, S., A. Lendlein, and F. Jung, "Developing standards and test protocols for testing the hemocompatibility of biomaterials," in *Hemocompatibility of Biomaterials for Clinical Applications*, pp. 51–76, Elsevier, 2018.
55. ISO, "Plastics – determination of tensile properties part 1: General principles," ISO ISO 527-1:2019(E), International Organization for Standardization, Geneva, Switzerland, 2019.